Chapter

Chaos and Complexity Dynamics of Evolutionary Systems

Lal Mohan Saha

Abstract

Chaotic phenomena and presence of complexity in various nonlinear dynamical systems extensively discussed in the context of recent researches. Discrete as well as continuous dynamical systems both considered here. Visualization of regularity and chaotic motion presented through bifurcation diagrams by varying a parameter of the system while keeping other parameters constant. In the processes, some perfect indicator of regularity and chaos discussed with appropriate examples. Measure of chaos in terms of Lyapunov exponents and that of complexity as increase in topological entropies discussed. The methodology to calculate these explained in details with exciting examples. Regular and chaotic attractors emerging during the study are drawn and analyzed. Correlation dimension, which provides the dimensionality of a chaotic attractor discussed in detail and calculated for different systems. Results obtained presented through graphics and in tabular form. Two techniques of chaos control, pulsive feedback control and asymptotic stability analysis, discussed and applied to control chaotic motion for certain cases. Finally, a brief discussion held for the concluded investigation.

Keywords: chaos, Lyapunov exponents, chaos indicator, bifurcation, topological entropy, correlation dimension

1. Introduction

Henri Poincaré, (1892–1908), [1], was first to acknowledge the possible existence of chaos in nonlinear systems while studying a 3-body problem comprising Sun, Moon and Earth. He noticed the dynamics of the system turned to be sensitive towards initial conditions, which was later termed as chaos. His results based on theoretical analysis and he could not demonstrate it because computers were not available at that time. Lorenz, a weather scientist, demonstrated existence of chaos by using a computer in 1963, [2], and in this way supported chaos theory of Poincaré. Thus, **Lorenz** provided the foundation of chaos theory and inspired a fundamental reappraisal of systems of nonlinearity in many disciplines of science, engineering, biological and medical sciences, atmospheric science, economics, social sciences and where not? In our everyday life, chaos happened frequently in various form like cyclone, tsunami, tornado, epidemics/pandemics etc. Spread of any uncontrollable form of disease in medical science is nothing but a chaotic and contagious nature of disease. Systematic studies in various areas resulting in numerous articles on chaos and nonlinear dynamics appeared in many well-reputed scientific journals, [3–19].

Most biological systems exhibit enormous diversity and structurally multicomponent resulting in ecological imbalance and disorder/disharmony in environment. Inspired by articles of Lotka, Volterra, and Allee, numerous articles appeared with diversity in assumptions depending of species and their living environmental conditions in predator-prey models, [20–44].

Real systems are mostly nonlinear and many of them are with multicomponent structure. Their individual elements possess individual properties. Such systems are termed as the complex system.

During evolution, a complex system exhibits chaos in some parameter space but also some other phenomena called complexity. This complexity is due to the interaction among multiple agents within the system displayed in the form of coexistence of multiple attractors, bistability, intermittency, cascading effects, exhibit of hysteresis properties etc. Thus, complexity can viewed as its systematic nonlinear properties and it is due to the interaction among multiple agents within the system. Foundation work and elaborate descriptions on complexity can viewed from some pioneer articles on complexity in nonlinear dynamics presented in [45–51]. Study of complexity means to know the results that emerging from a collection of interacting parts.

A dynamical system be chaotic then it must be (i) sensitive to initial conditions, (ii) topologically mixing and (iii) its periodic orbits must be dense. In chaotic systems, there exists a strange attractor, a chaotic set, which has fractal structure. Complex systems are also sensitive to their initial conditions and two complex systems that are initially very close together in terms of their various elements and dimensions can end up in distinctly different places. Wide discussions on complex system may found in some pioneer literatures, [14, 18, 45, 46, 48, 50, 51].

Chaos measured by Lyapunov exponents, (also called Lyapunov characteristic components or LCEs); LCE > 0 indicates existence of chaos and LCE < 0 indicates regularity, [52–62]. A complex system can better understood by measuring (i) chaos, (ii) Topological entropies and (iii) correlation dimension. Topological entropy, a non-negative number, provides a perfect way to measure complexity of a system. More topological entropy in any system signifies more complexity in it. Actually, it measures the evolution of distinguishable orbits over time, thereby providing an idea of how complex the orbit structure of a system is, [48–50, 61–69]. A system may be chaotic with zero topological entropy. In addition, a significant increase in topological entropy does not justify that it is chaotic. The book by Nagashima and Baba, [62], gives a very clear definition of topological entropy. The correlation dimension provides the dimensionality of the chaotic attractor. Correlation dimensions are non-integers and this is one reasons besides self-similarity that chaotic sets have fractal structure, [60, 68–73].

It emerges from a good number of recent researches that chaos appearing in dynamical system be controlled and suggested number techniques to control chaos, [74–88]. These techniques have some limitations depending on the models and nature of nonlinearity.

Objective of this article is to investigate the emergence of chaos and complexity in nonlinear dynamical systems through examples of nonlinear models. Numerical simulations carried out for bifurcation analysis, plotting of LCEs and topological entropies for different systems. Numerical calculations extended to obtain correlation dimensions for certain chaotic attractors emerging in different systems. The study further extended to explain different types of chaos controlling technique. Studies confined to one, two and three-dimensional systems only.

2. Dynamic models with chaos and complexity

2.1 One dimensional discrete models

2.1.1 Dynamics of laser map

A highly simplified type discrete nonlinear model for laser system, arising from Laser Physics, described in articles, [12, 50, 89–91]. The model describes evolution of certain Fabry-Perot cavity containing a saturable absorber and driven by an external laser represented by

$$x_{n+1} = Q - \frac{A\, x_n}{1 + {x_n}^2}, \forall \in \Re, n \in N \tag{1}$$

Here Q is the normalized input field and A is a parameter depends on the specifics of the parameters and $A > 0$. The fixed points of the map are the real root of equation

$$x^3 - Qx^2 + (1 + A)x - Q = 0 \tag{2}$$

This equation has either three real roots or one real and a pair of complex conjugate roots depending on parameter space (A, Q). Stability occur in the form of stability and bistability, [89].

Fixed Points and Bifurcations:

For Q fixed, $Q = 2.76$, and $A < 4.3793$, only one stable steady state solution exits and stable two cycle starts when A exceeds this value. Thus, approximately, $A = 4.3793$, is the bifurcation point. At value $A = 4.3$, the stable steady state solution is $x^* = 0.720533$.

Keeping $Q = 2.76$ and varying parameter A, bifurcation diagrams are drawn, **Figure 1**, for four different ranges of values of A. Similarly, keeping A fixed,

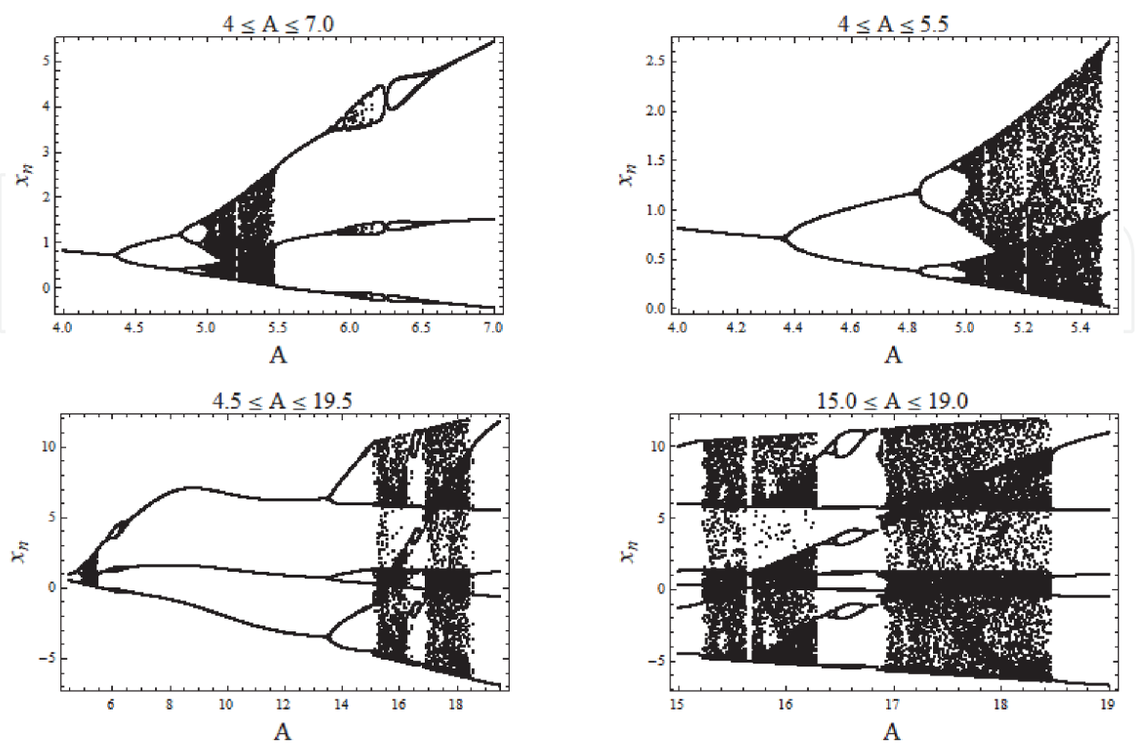

Figure 1.
Bifurcation diagrams of map (1) for four cases: when Q = 2.76 and parameter A varies.

$A = 5.4$ and varying Q in four different ranges, bifurcation diagrams are drawn, **Figure 2**. One observe clearly the appearance of periodic windows within chaotic region of bifurcations as an indication of intermittency and other complex phenomena. Periodic windows become gradually shorter and appearance become more frequent while moving forward in parameter space.

Both time series plots shown in **Figure 3** are for chaotic evolution of system (1) and correspond to parameters (a) (A, Q) = (5.3, 2.76), due to which an unstable fixed point obtained as $x^* = 0.58531$, and parameters (b)) (A, Q) = (5.4, 2.9), due to which an unstable fixed point obtained as $x^* = 0.572218$. For both cases, initial point taken is $x_0 = 0.5$ which lies nearby these points and so, also, unstable.

Calculations of Lyapunov Exponents, (LCEs):

Lyapunov exponents, LCEs, for map (1), calculated for four cases, **Figure 4**, positive LCEs appearing above zero line clearly indicate chaotic motion and those below this line indicate regular motion.

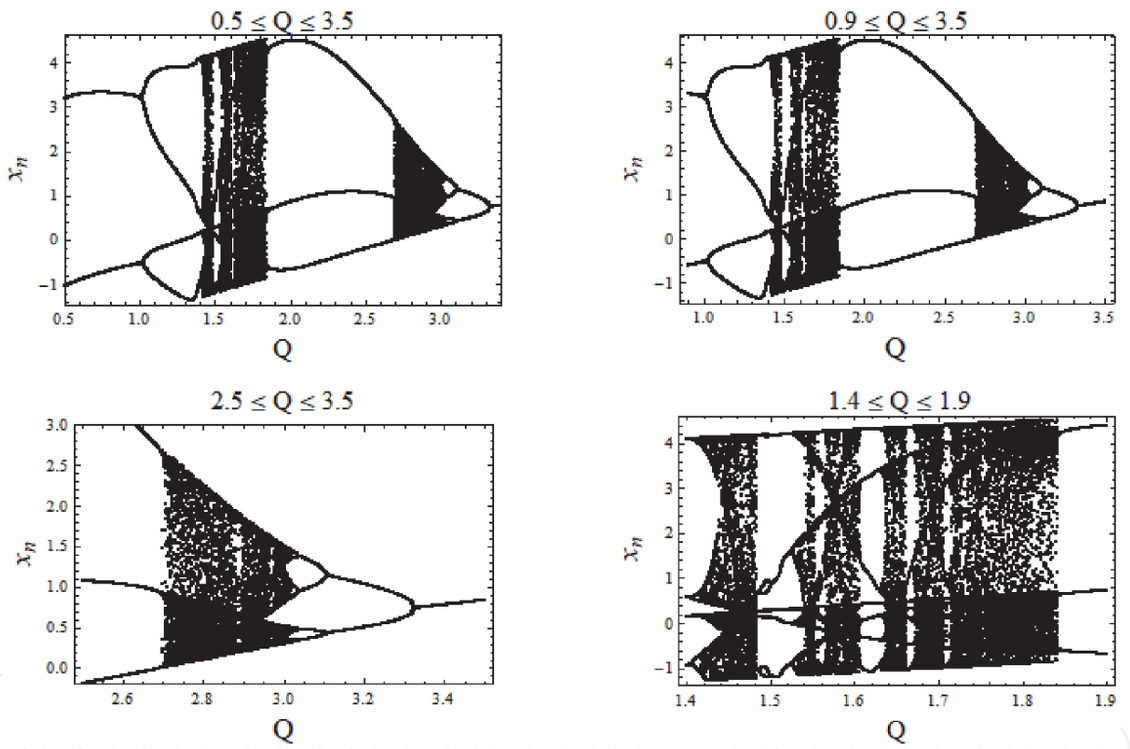

Figure 2.
Bifurcation diagrams of map (1) for four cases: when A = 5.4 and parameter Q varies.

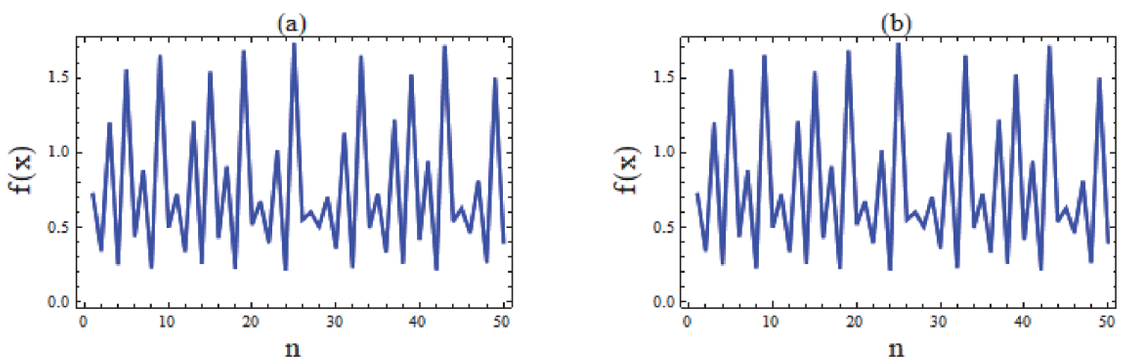

Figure 3.
Chaotic time series plots with initial value $x_0 = 0.5$: (a) A = 5.3, Q = 2.76 and (b) A = 5.4, Q = 2.9.

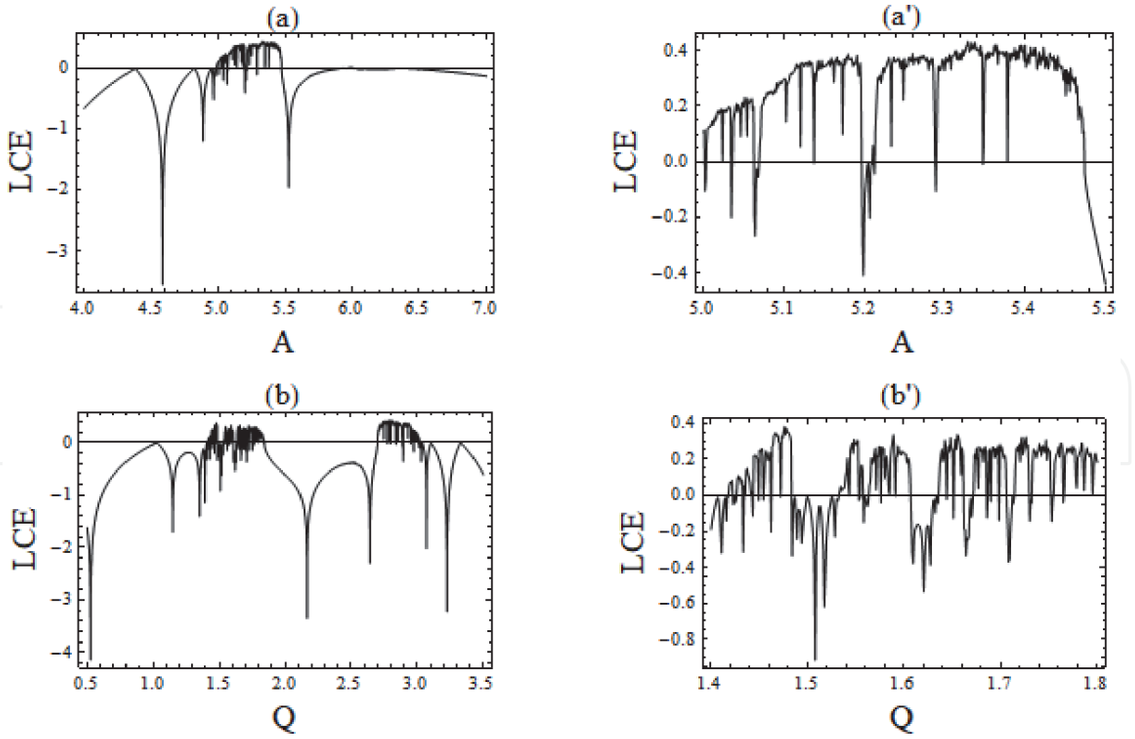

Figure 4.
Plots of LCEs: (a) for the upper row Q = 2.76, 4.0 ≤ A ≤ 5.5 and 5.0 ≤ A ≤ 7.0; (b) for the lower row A = 5.4, 0.5 ≤ Q ≤ 3.5 and 1.4 ≤ Q ≤ 1.8.

Topological Entropies:

Numerical calculations further proceeded to calculate topological entropies for system (1) and shown in **Figure 5**; where figures of upper row obtained by varying parameter A while keeping parameter Q = 2.76 and those of lower row obtained by varying parameter Q while keeping parameter A = 5.4.

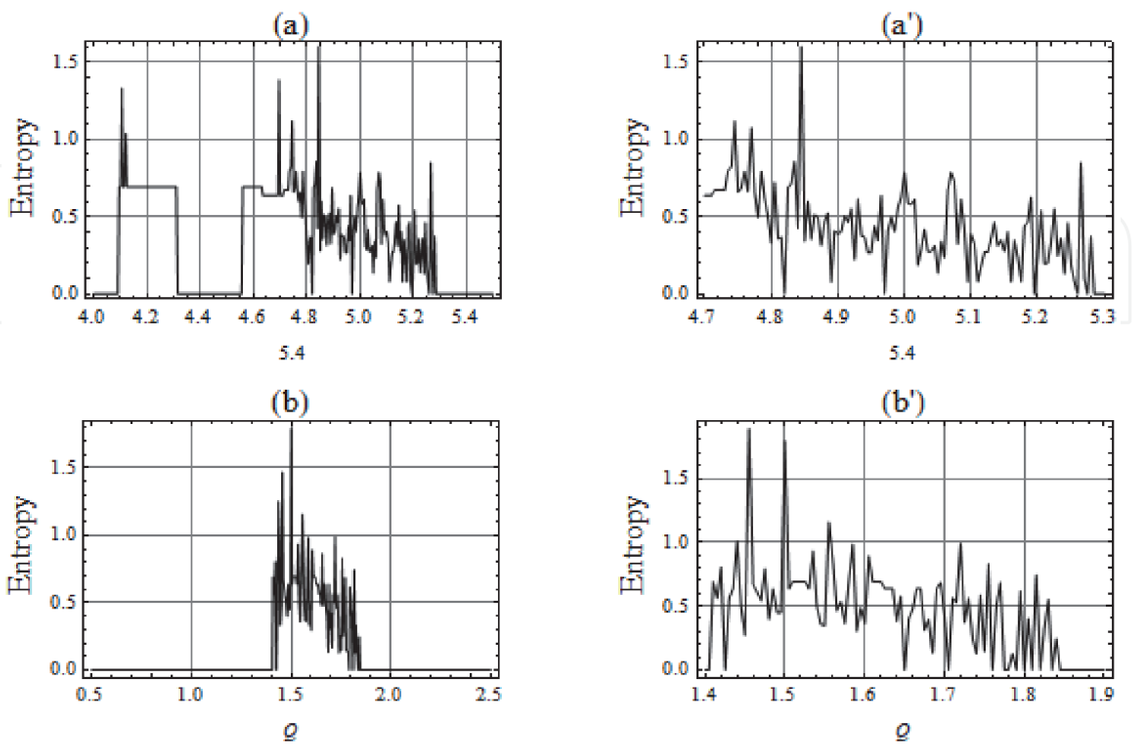

Figure 5.
Topological entropy plots: (a) for upper row Q = 2.76 and 4.0 ≤ A ≤ 5.5 & 4.7 ≤ A ≤ 5.3; (b) for lower row A = 5.4 and 0.4 ≤ Q ≤ 2.5 & 1.4 ≤ Q ≤ 1.9.

Correlation Dimension:

Extending further the numerical study, correlation dimensions of system (1) calculated for a chaotic attractor by using Mathematica codes, [73].

Consider an orbit $O(\boldsymbol{x_1}) = \{x_1, x_2, x_3, x_4 \ldots \ldots\}$, of a map $f : U \to U$, where Us an open bounded set in R^n. To compute correlation dimension of $O(x_1)$, for a given positive real number r, we form the correlation integral,

$$\mathrm{C(r)} = \lim_{\mathrm{n}\to\infty} \frac{1}{\mathrm{n}\,(\mathrm{n}+1)} \sum_{\mathrm{i}\neq\mathrm{j}}^{\mathrm{n}} \mathrm{H}\left(\mathrm{r} - \|\mathbf{x_i} - \mathbf{x_j}\|\right) \tag{3}$$

Where,

$$\mathrm{H(x)} = \begin{cases} 0, & \mathrm{x} < 0 \\ 1, & \mathrm{x} \geq 0 \end{cases}$$

is the unit-step function, (Heaviside function). The summation indicates number of pairs of vectors closer to r when$1 \leq \mathrm{i}, \mathrm{j} \leq \mathrm{n}$ and $i \neq j$. C(r) measures the density of pair of distinct vectors $\mathbf{x_i}$ and $\mathbf{x_j}$ that are closer to r.

The correlation dimension $\mathrm{D_c}$ of $\mathrm{O}(\mathbf{x_1})$ is then defined as

$$\mathrm{D_c} = \lim_{\mathrm{r}\to 0} \frac{\log \mathrm{C(r)}}{\log \mathrm{r}} \tag{4}$$

To obtain $\mathrm{D_c}$, $\log \mathrm{C(r)}$ is plotted against $\log r$, **Figure 6**, and then we find a straight line fitted to this curve. The intercept of this straight line on y-axis provides the value of the correlation dimension $\mathrm{D_C}$. Correlation dimensions of time series attractors, **Figure 3**, obtained as:

a. For first attractor, Q = 2.76, A = 5.3, a plot of the correlation integral curve is shown in **Figure 6**. Then, the linear fit of the correlation data used in this figure obtained as

$$y = 0.95661x + 0.687605$$

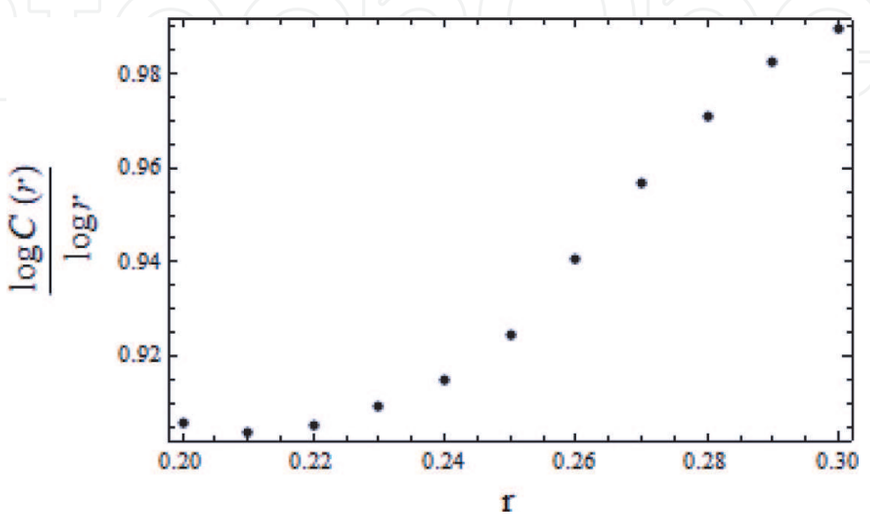

Figure 6.
Plot of correlation integral curve for A = 5.3, Q = 2.76 and x_o = 0.5.

The y-intercept of this straight line is 0.687605. Therefore the correlation dimension of the attractor in this case is $D_C = 0.69$.

b. In a similar way, correlation dimension for second attractor of **Figure 3**, A = 5.4 and Q = 2.9, as $D_c = 0.56$. Plots of correlation dimensions against parameters A, Q shown in **Figure 7**.

2.1.2 Dynamics of biological red cells model

The population of red blood cells in a healthy human being oscillates within a certain tolerance interval in normal circumstances. But, sometimes, in presence of a disease such as anemia, this behavior fluctuate dramatically. A discrete model of blood cell populations, Martelli, ([73], p: 35), presented here.

Let x_n, x_{n+1} representing quantities of cells per unit volume (in millions) at time n and $n+1$, respectively and p_n, d_n are, respectively, the number of cells produced and destroyed during the nth generation then

$$x_{n+1} = x_n + p_n - d_n \tag{5}$$

Then, assuming that

$$d_n = a\, x_n, a \in [0,1]$$
$$p_n = b(x_n)^r e^{-s x_n},$$

where b, r, s all positive parameters. With these our one-dimensional discrete model for blood cells populations comes as

$$x_{n+1} = (1-a)\, x_n + b\, (x_n)^r e^{-s\, x_n} \tag{6}$$

The case $a = 1$, means that during the time interval under consideration all cells that were alive at time n are destroyed. In such a case, above models simply comes as

$$x_{n+1} = b(x_n)^r e^{-s\, x_n} \tag{7}$$

For $a = 0.8, b = 10$, $r = 6$ and $s = 2.5$, three fixed points $x^*{}_0 = 0, x^*{}_1 = 0.989813$, $x^*{}_2 = 3.53665$ obtained for system (6) of which only $x_0^* = 0$ is stable and other two are unstable. Chaotic motion observed for values of parameter $a = 0.8, b = 10, r = 6, s = 2.5$, as shown in the time series plot, **Figure 8**, with initial condition $x_0 = 1.5$.

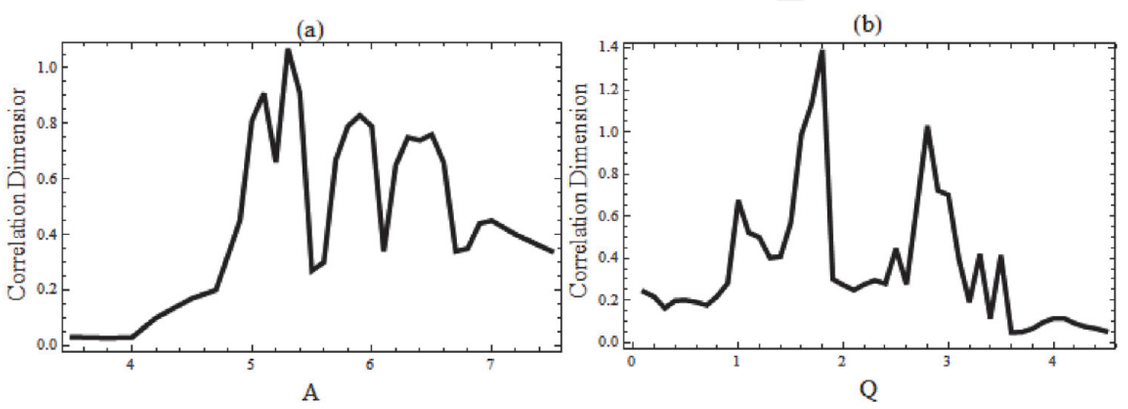

Figure 7.
Plots of correlation dimensions: (a) with Q = 2.76 and varying A, (b) with A = 5.4 and varying Q.

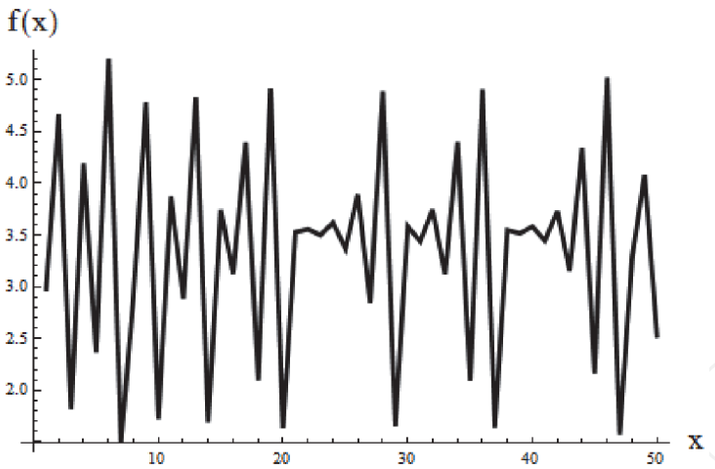

Figure 8.
Chaotic time series plot of map (6) for $a = 0.8$, $b = 10$, $r = 6$, $s = 2.5$ and $x_0 = 1.5$.

Interesting bifurcations observed for this map: For $b = 1.1 \times 10^6$, $r = 8$, two bifurcation diagrams are drawn; (a) in one for s =16 and $0 \le a \le 1$, and (b) in another for $a = 0.8$ and $3.5 \le s \le 16.0$ and shown in **Figure 9**. In former case one finds initially period doubling bifurcation followed by loops before emergence of chaos. In later case, one finds some typical type of bifurcation showing chaos adding, folding and the bistability like phenomena. A magnification of right figure, **Figure 10**, for smaller range, $4.5 \le s \le 8.5$, justifying chaos adding behavior.

Regular and chaotic motion experienced through bifurcation diagrams, **Figures 9** and **10**, again confirmed by plots of Lyapunov exponents, **Figure 11**. This system, bears enough complexity and, as its measure, plot of topological entropies, **Figure 12**, obtained for values $r = 6$, $s = 16$ and $b = 1.1 \times 10^6$ and $0 \le a \le 1$. Fluctuations in increase of topological entropies appear, approximately, in the region $0.25 \le a \le 0.95$ indicate existence of complexity.

The correlation dimension of its chaotic attractor for values $a = 0.78$, when $r = 6$, $s = 16$ and $b = 1.1 \times 10^6$ is obtained as $D_c \cong 0.253$.

2.2 Two-dimensional models

2.2.1 Two-Gene Andrecut-Kauffman System

Chaos and complexity study of a discrete two-dimensional map for two-gene system, proposed by Andrecut and Kaufmann, investigated recently, [35, 71, 92]. The map used to investigate the dynamics of two-gene system for chemical

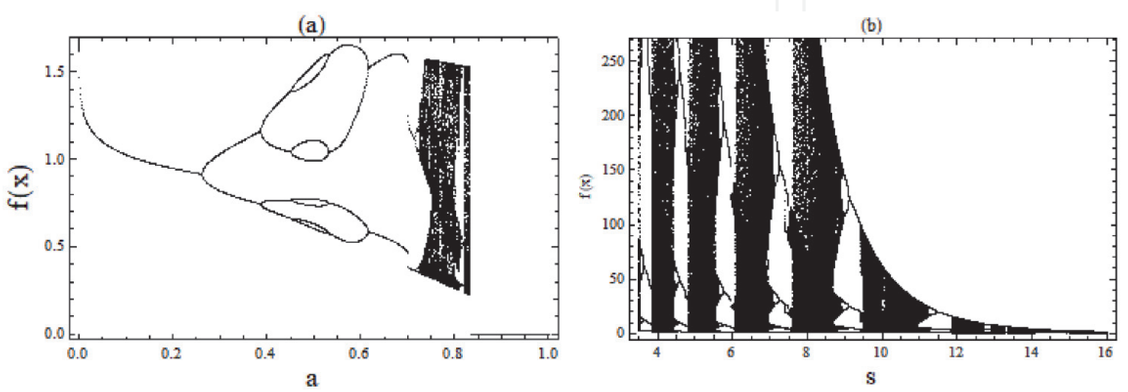

Figure 9.
Bifurcation plots of Blood Cell model for $= 8$, $b = 1.1 \times 10^6$ then for (a) $s = 16$ and $0 \le a \le 1$ and for (b) $a = 0.1$ and $3.5 \le s \le 16$.

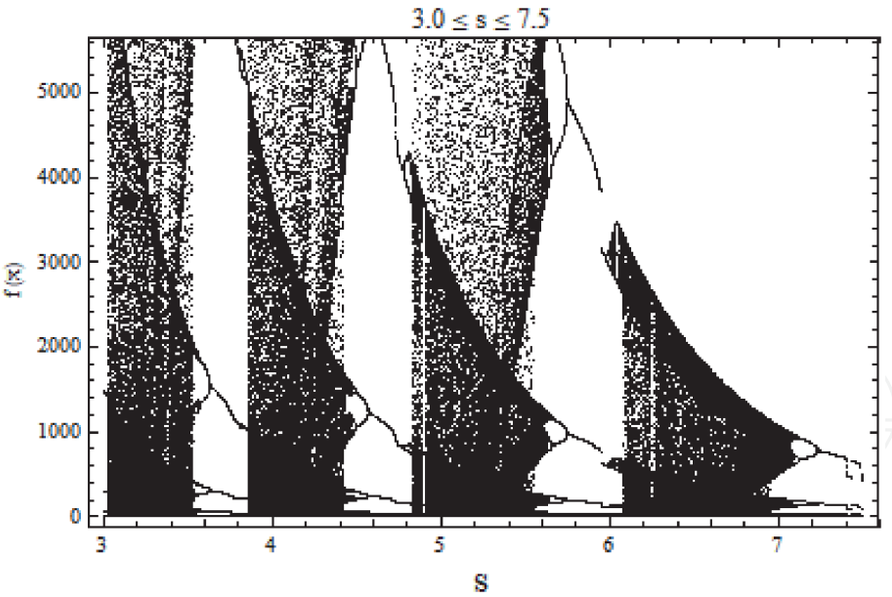

Figure 10.
Bifurcation of Blood Cell model when $3.0 \leq s \leq 7.5$ *and* $a = 0.8,\ r = 8,\ b = 1.1 \times 10^6$.

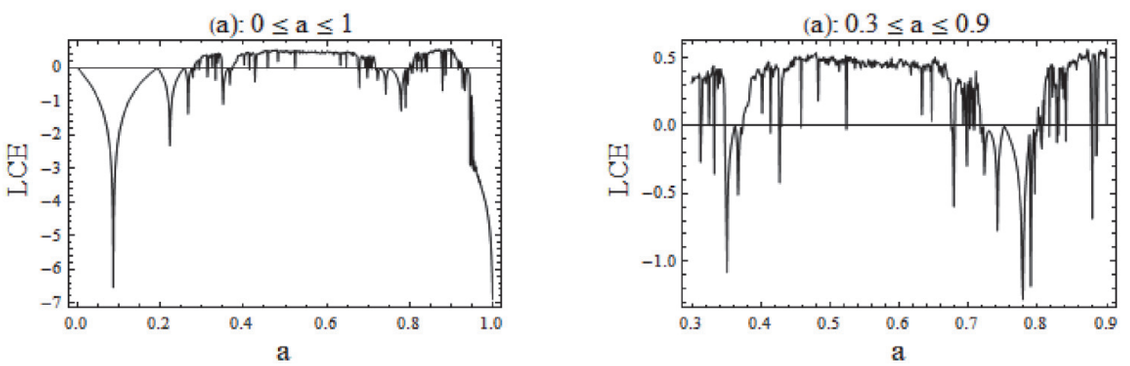

Figure 11.
LCE Plots for $= 6$, $s = 16$ *and* $b = 1.1 \times 10^6$, *negative and positive values of LCEs, respectively, below and above the zero line show the regular and chaotic zones of parameter space.*

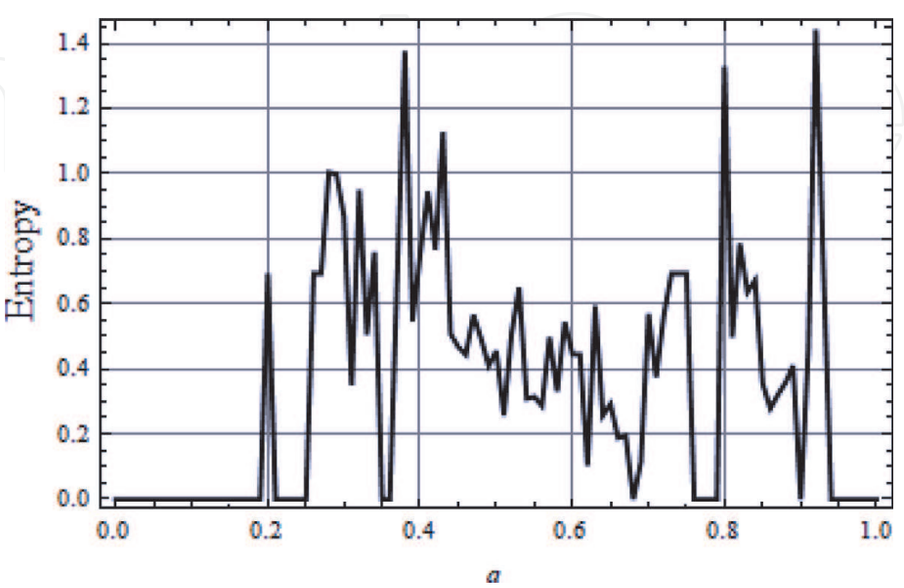

Figure 12.
Topological entropy plot for $r = 6, s = 16$ *and* $b = 1.1 \times 10^6$ *and* $0 \leq a \leq 1$.

reactions corresponding to gene expression and regulation. The discrete dynamic variables x_n and y_n describe the evolutions of the concentration levels of transcription factor proteins. The map represented by following pair of difference equations:

$$x_{n+1} = \frac{a}{1 + (1-b)\, x^t_n + b\, y^t_n} + c\, x_n$$
$$y_{n+1} = \frac{a}{1 + (1-b)\, y^t_n + b\, x^t_n} + d y_n \qquad (8)$$

With parameter values $a = 25$, $b = 0.1$, $c = d = 0.18$ and $t = 3$, one obtains four different fixed points with coordinates (2.30409, 2.30409), (−2.52688, 2.44162), (2.44162, −2.52866), (−2.39464, −2.39464) and all are unstable.

For $c \neq d$ and when $a = 25, b = 0.1, c = 0.18, d = 0.42$, and $t = 3$, again, four unstable fixed points exists as (2.2832, 2.5413), (−2.5458, 2.6566), (2.4613, −2.7288), (−2.3744, −2.61705).Therefore, for all these the cases, orbit with initial point taken nearby any of the fixed points be unstable and may be chaotic also.

We intend to investigate certain dynamic behavior of system (8) for cases when $c = d$ and when $c \neq d$ of evolutions showing irregularities due to presence of chaos and complexity.

Numerical Simulations:

Drawing bifurcation diagrams and calculating Lyapunov exponents, topological entropy and correlation dimensions of the system for different cases have investigated performing numerical simulations. For values of the control parameters following ranges proposed: $a \in [0, 50]$, $c \in [-0.4, 0.4]$, $b = 0.1$, $d = 0.5$, $t = 3, 4, 5$.

Case 1: Taking $c = d$, bifurcation diagrams are drawn along the directions x and y, by varying c for cases t = 3, 4, 5 and certain fixed values of other parameters as shown in **Figure 13**. Then, plots of attractors have been obtained for parameters $a = 25, b = 0.1, t = 3$ and (i) for regular case $c = d = 0.32$ and (ii) for chaotic case $c = d = 0.18$ and shown in **Figure 14**. In each case when t = 3, 4, 5, bifurcations show period doubling leading to chaos and then to regularity. Also, bistability and folding nature of phenomena are appearing here.

Lyapunov Exponents & Topological Entropies:

For chaotic evolution, when $a = 25, b = 0.1, t = 3, c = d = 0.18$, Lyapunov exponents are obtained shown in **Figure 15**. Numerical investigations further proceeded for calculation of topological entropies. In **Figure 16**, plots of topological entropies are presented for t = 3, 4, 5 and for different ranges of parameter c. Analysis of these plots, gives an impression that for the case t = 3, system shows enough complexity in the range $0.05 \leq c \leq 0.23$. For the case t = 4, the system shows high complexity in the range $0 \leq c \leq 0.22$ and in case t = 5, high complexity appears in $0 \leq c \leq 0.44$.

Case II: When c and d are different, bifurcation diagrams, **Figure 17**, shows clear picture of complex nature of the system.

In **Figure 18**, plots of Lyapunov exponents, (LCE's), for chaotic evolution for different cases discussed above are shown in the upper row and plots of topological entropies are shown in the lower row for these cases. For all the plots, parameters a = 25 and b = 0.1 are common. Here, topological entropy plots are drawn for different ranges of parameter c.

When parameters c and d both were allowed to vary, one gets 3D plots for topological entropies as shown here in **Figure 19**.

Correlation dimensions:

Being one of the characteristic invariants of nonlinear system dynamics, the correlation dimension provides measure of dimensionality for the underlying attractor of the system. A statistical method used to determine correlation dimension. It is

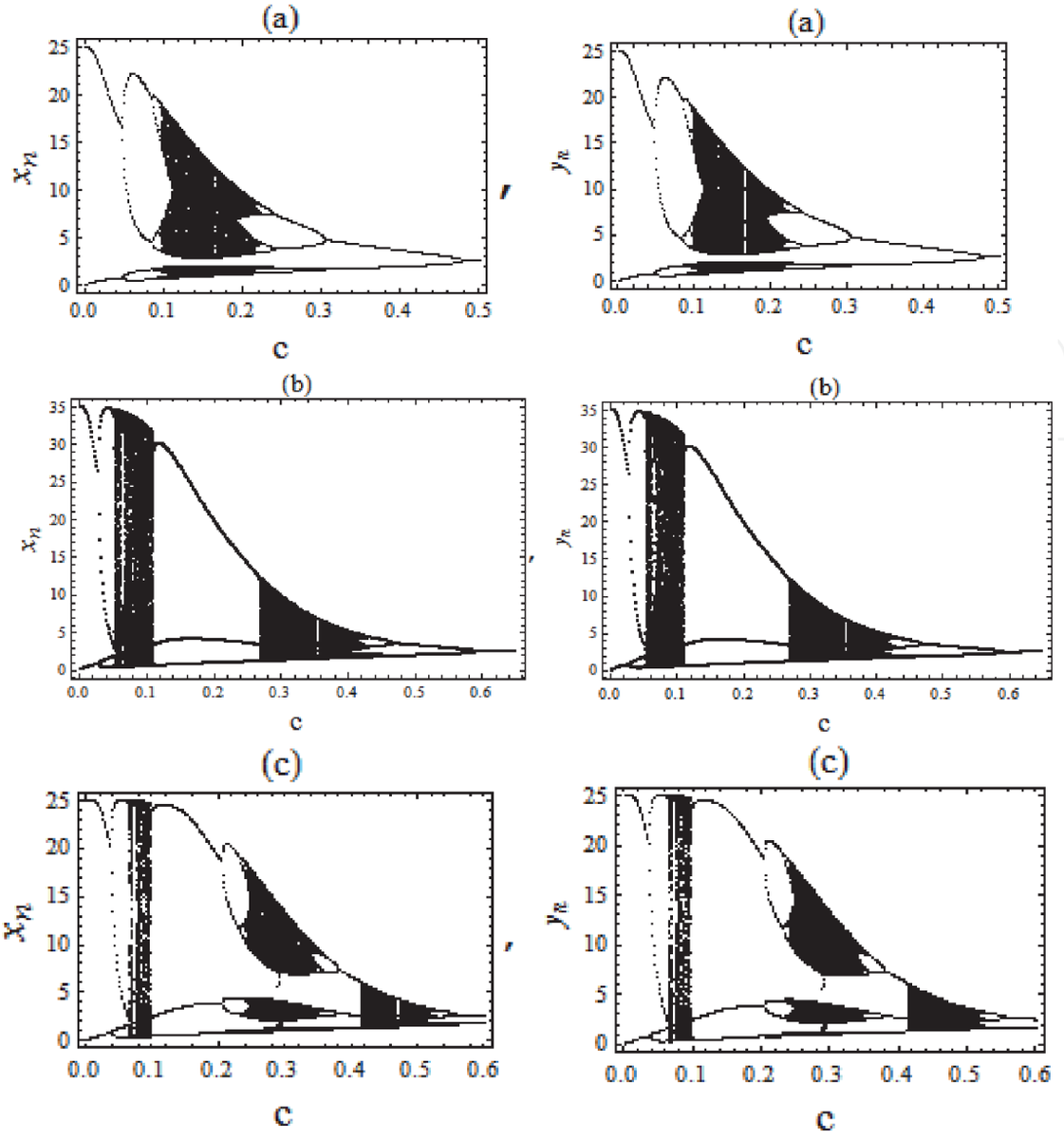

Figure 13.
Three cases of bifurcation scenarios of map (8) for parameters $c = d$: (a) t= 3, $a = 25, b = 0.1$ and $0 \leq c \leq 0.5$; (b) t = 4, $a = 35, b = 0.1$ and $0 \leq c \leq 0.65$; (c) t = 5, $a = 25, b = 0.1$ and $0 \leq c \leq 0.5$.

an efficient and practical method in comparison to others, like box counting etc. The procedure to obtain correlation dimension follows from steps of calculations in [73]:

For case t = 3 and a = 25, b = 0.1, c = 0.28, d = 0.12, correlation integral data calculated and its plot is obtained, **Figure 20**. The linear fit of correlation integral data obtained as

$$Y = 0.0581323x - 0.580866$$

The y-intercept of this straight line is 0.580866. Therefore the correlation dimension of the attractor in this case is, approximately, D_c = 0.581.

Computation of correlation dimension carried out for more cases for different set of values of parameters as shown in **Table 1**.

2.2.2 Complexities in micro-economic Behrens Feichtinger model

Investigation on microeconomic chaotic disturbances and certain measure to control chaos appeared in some recent articles, [72, 93–95], extended here for

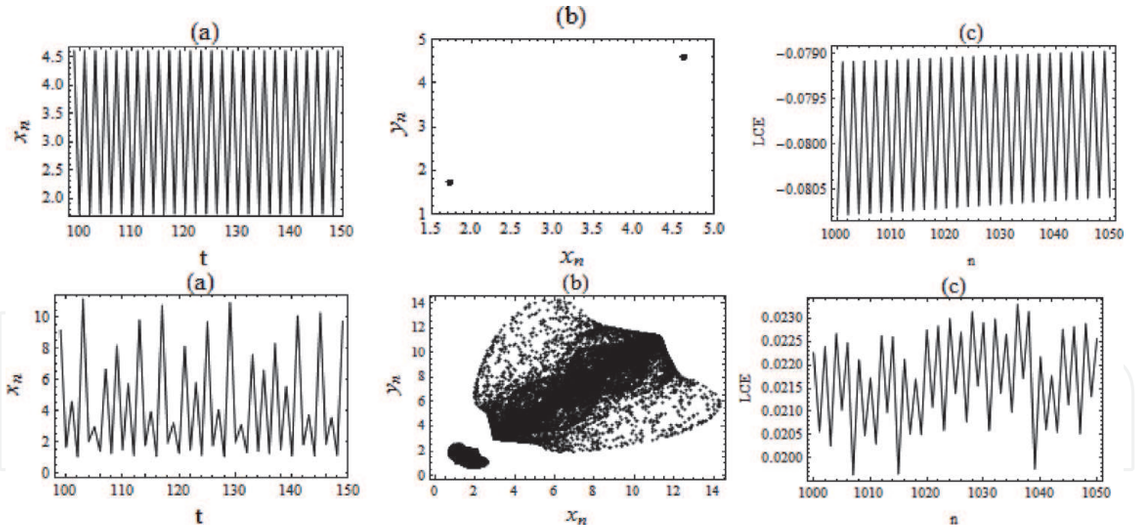

Figure 14.
Figures (a), (b), (c) correspond to time series, phase plane attractors and Lyapunov exponents; upper row is for regular case and the lower row is for chaotic case of map (8). Parameters values are taken as $a = 25, b = 0.1, t = 3$ *and (i) for regular case* $c = d = 0.32$ *and (ii) for chaotic case* $c = d = 0.18$.

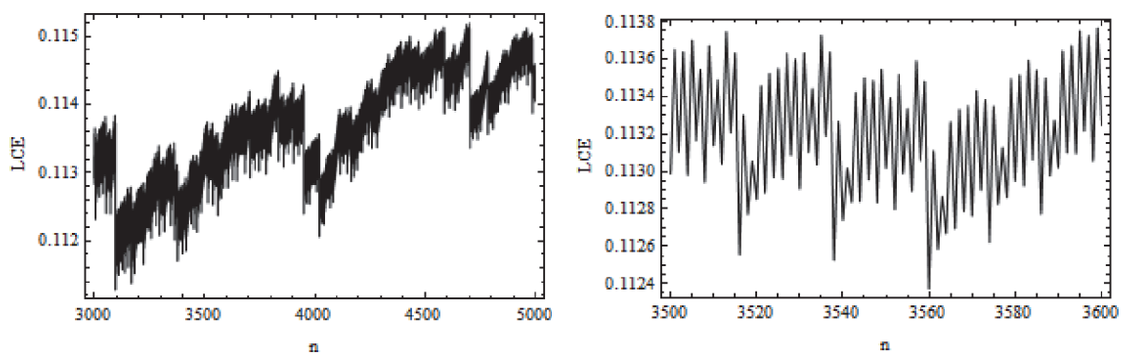

Figure 15.
Plots of Lyapunov exponents for chaotic evolution of map (8). Parameters are $a = 25, b = 0.1, t = 3, c = d = 0.18$ *and when evolving from initial point (2.1, 2.1).*

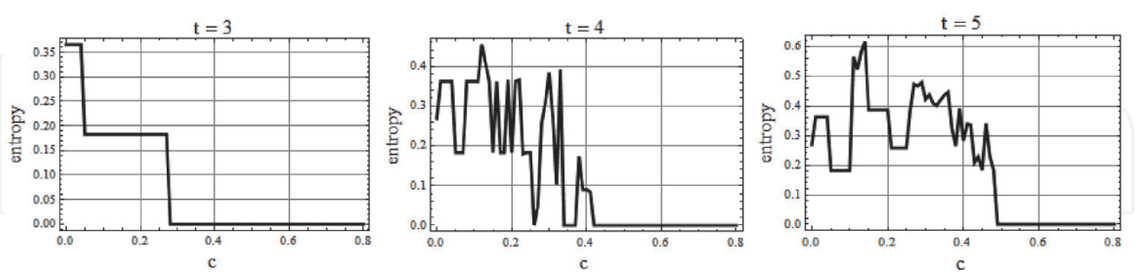

Figure 16.
Plots of topological entropy for map (8) when parameter $c = d$. *From left: (i)* $t = 3$, $a = 25, b = 0.1$ *and* $0 \leq c \leq 0.5$; *(ii)* $t = 4$, $a = 35, b = 0.1$ *and* $0 \leq c \leq 0.65$; *(iii)* $t = 5$, $a = 25, b = 0.1$ *and* $0 \leq c \leq 0.8$.

complexity analysis. The problem proposed as an micro economic model of two firms X and Y competing on the same market of goods having asymmetric strategies. The sales x_n and y_n of both firms are evolving in discrete time steps.

$$x_{n+1} = (1 - \alpha)\, x_n + \frac{a}{1 + e^{[-c\,(x_n - y_n)]}}$$

$$y_{n+1} = (1 - \beta)\, y_n + \frac{b}{1 + e^{[-c\,(X_n - Y_n)]}} \tag{9}$$

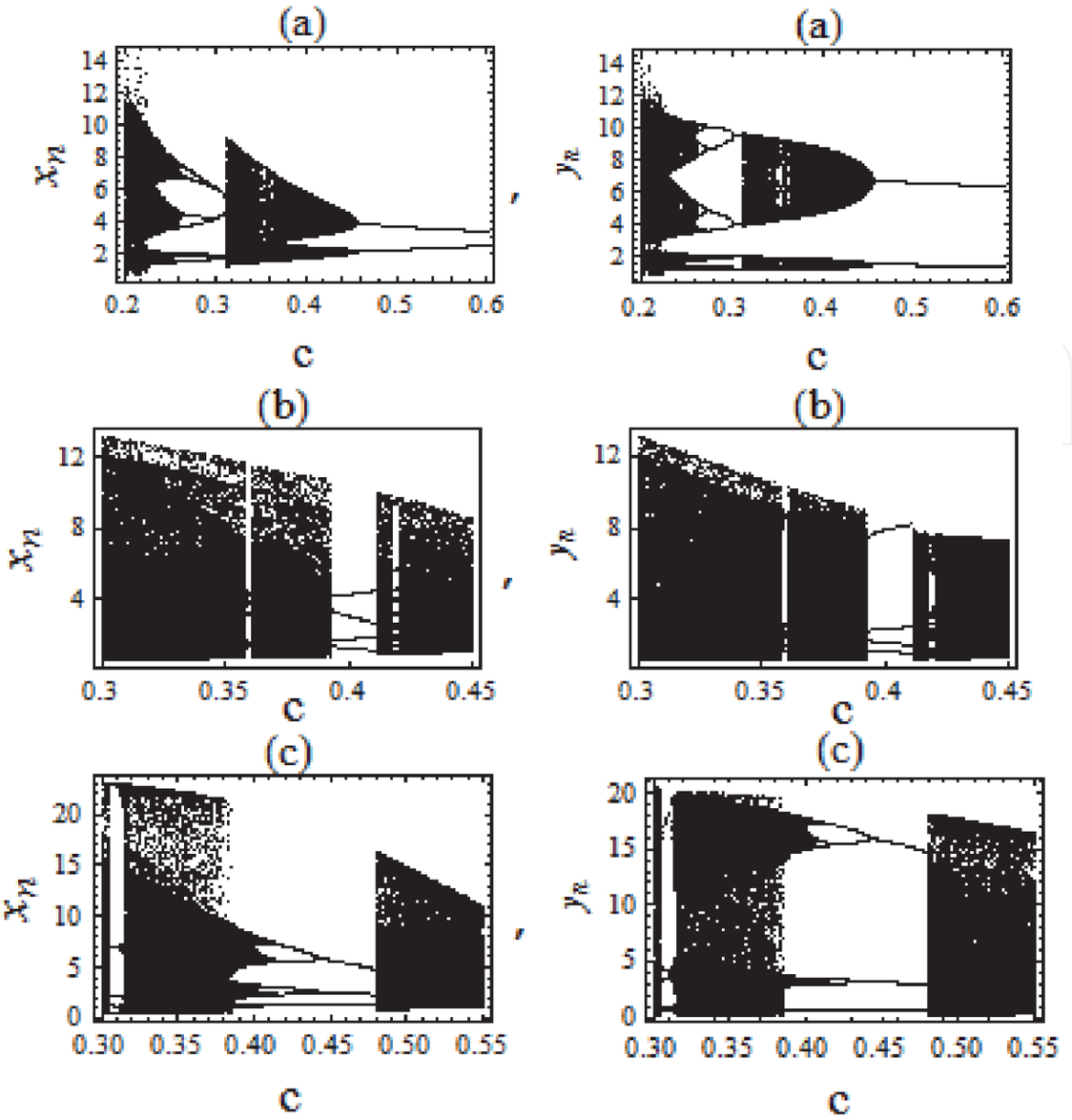

Figure 17.
Bifurcation plots when $c \neq d$ for different ranges of parameter c. Cases (a), (b), (c), corresponds to t = 3, t = 4, t = 5. Parameters are $a = 25, b = 0.1$ and $d = 0.20$ for plots (a) & (c) and d = 0.30 for plot (b).

where α, β $(0 < \alpha, \beta < 1)$ are the time rates at which the sales of both firm decays in the absence of investments. Parameters a, b describe the investment effectiveness of both the firms. Parameter c is an "elasticity" measure of the investment strategies. For parameter values $\alpha = 0.46$, $\beta = 0.7$, $a = 0.16$, $b = 0.9$, $c = 105$, we have observed the chaotic attractor of this model.

Bifurcation Diagram:

Bifurcation diagrams for system (9) obtained for $\alpha = 0.46$, $\beta = 0.7$, $a = 0.16$, $b = 0.9$ and by varying parameter c, $8 \leq c \leq 160$ and in close range, $6 \leq c \leq 8$, **Figure 21**. Then, again it obtained for values $\alpha = 0.46$, $\beta = 0.7$, $a = 0.16$, $b = 0.6$, $c = 110$ and $0 \leq a \leq 0.4$, **Figure 22**. Appearance of period doubling followed by chaos visible from these figures.

Attractors:

Time series plots and a plot of chaotic attractor obtained for values $a = 0.16$, $b = 0.9$, $c = 105$, $\alpha = 0.46$, $\beta = 0.7$ of system (9) shown in **Figure 23**. Plots shown in **Figure 24** are of LCEs for the chaotic motion.

Topological Entropies: Topological entropies calculated numerically and plotted. These are shown in **Figure 25**. One finds significant increase topological

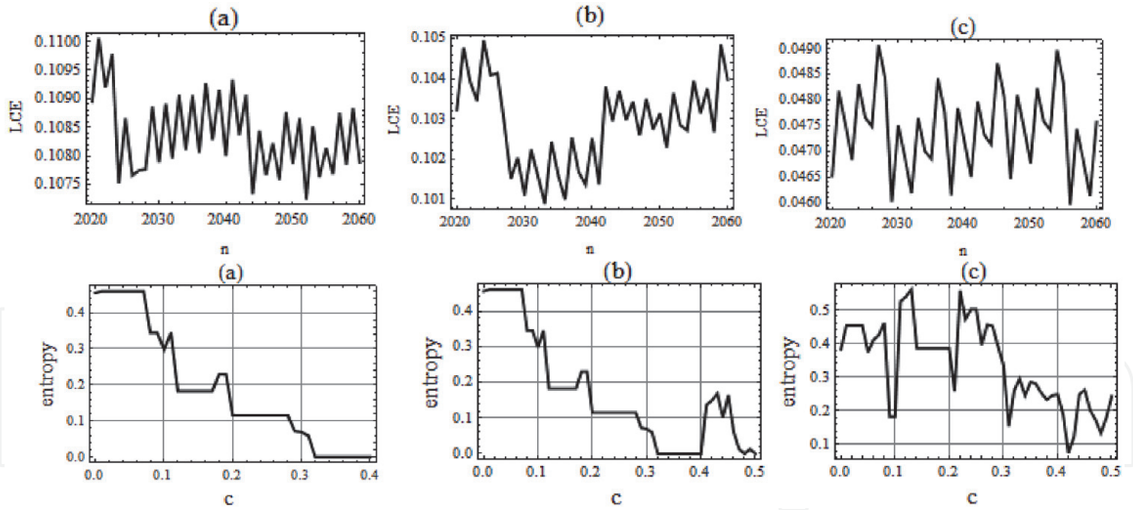

Figure 18.
Upper row plots are for LCE's and lower row plots are for topological entropies. Plots with (a), (b), (c) are respectively corresponds to the cases t = 3, 4, 5. Parameters a = 25, b = 0.1 are common for all the plots. Then, for (b) & (c) LCE's plots, c = 0.2, d = 0.15 and that for plot (c) , c = 0.28, d = 0.12. For lower row topological entropy plots, except parameter t, parameters a = 25, b = 0.1, d = 0.15 are common for all.

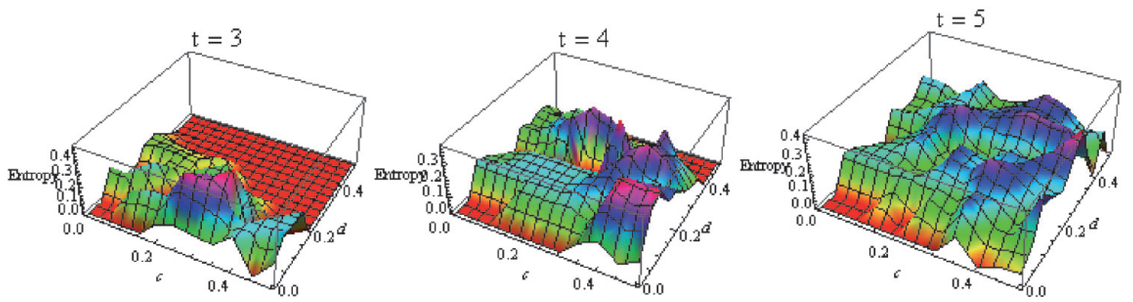

Figure 19.
3D plots for topological entropy variations. Parameters values are taken as a = 25, b = 0.1 and then 0 ≤ c ≤ 0.5 & 0 ≤ d ≤ 0.5.

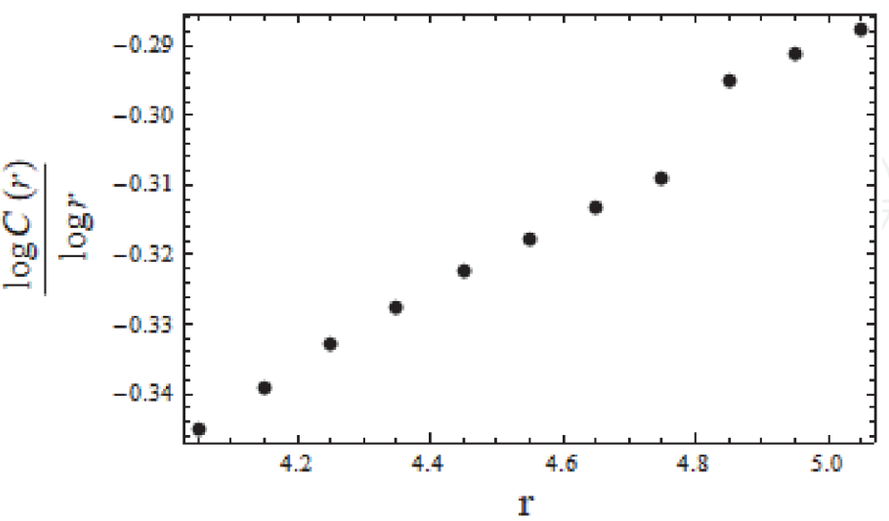

Figure 20.
Plot of correlation integral curve for t = 3 and a = 25, b = 0.1, c = 0.28, d = 0.12.

entropy where the system shows regularity, (e.g., $20 \leq c \leq 75$), and for values α = 0.46, β = 0.7, a = 0.16 and b = 0.9. This shows presence of complexities though there is no chaos.

Cases (t)/Parameters	a	b	c	d	Approximate D_c
t = 3	25	0.1	0.28	0.12	0.581
t = 4	25	0.1	0.18	0.18	0.645
t = 5	25	0.1	0.18	0.18	0.703
t = 4	25	0.1	0.28	0.12	0.676
t = 5	25	0.1	0.28	0.12	0.772
t = 3	35	0.1	0.2	0.2	0.877
t = 4	35	0.1	0.2	0.2	0.618
t = 5	35	0.1	0.2	0.2	1.264

Table 1.
Correlation Dimensions for different sets of parameters.

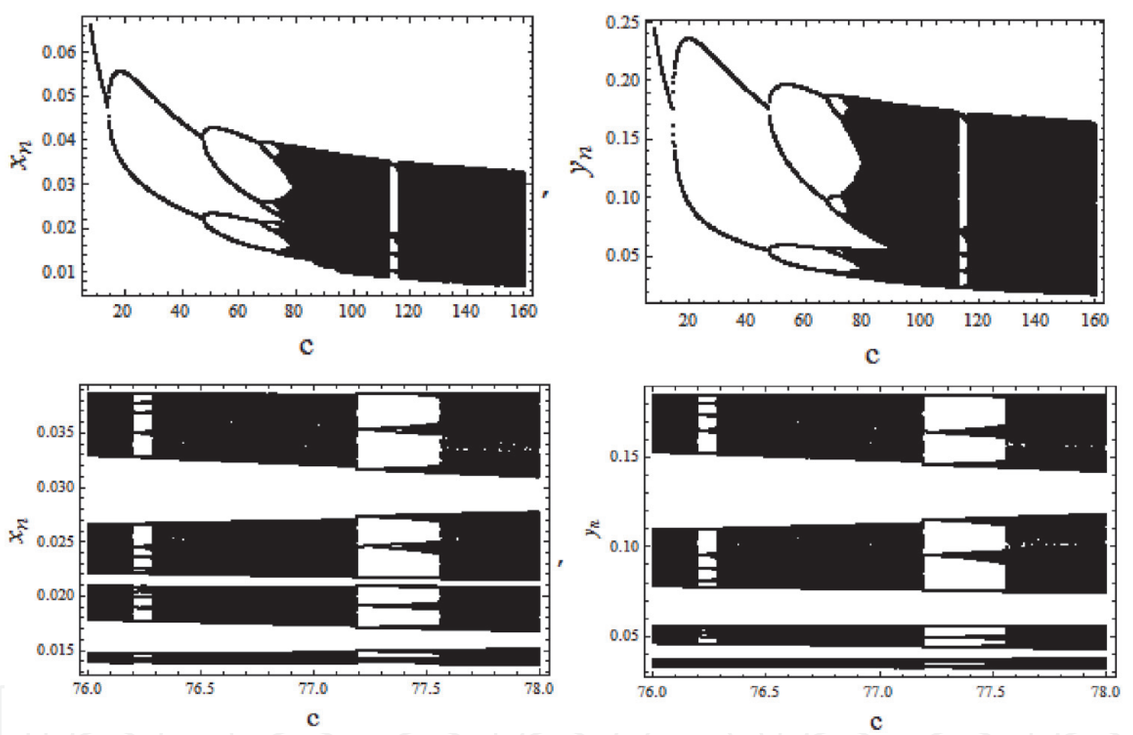

Figure 21.
Bifurcation diagrams of system (9) with respect to coordinates x and y. Lower plots are correspond to bifurcations in close range to indicate the appearance of periodic windows within bifurcation. $\alpha = 0.46$, $\beta = 0.7$, $a = 0.16$, $b = 0.9$, $8 \leq c \leq 160$ & $6 \leq c \leq 8$.

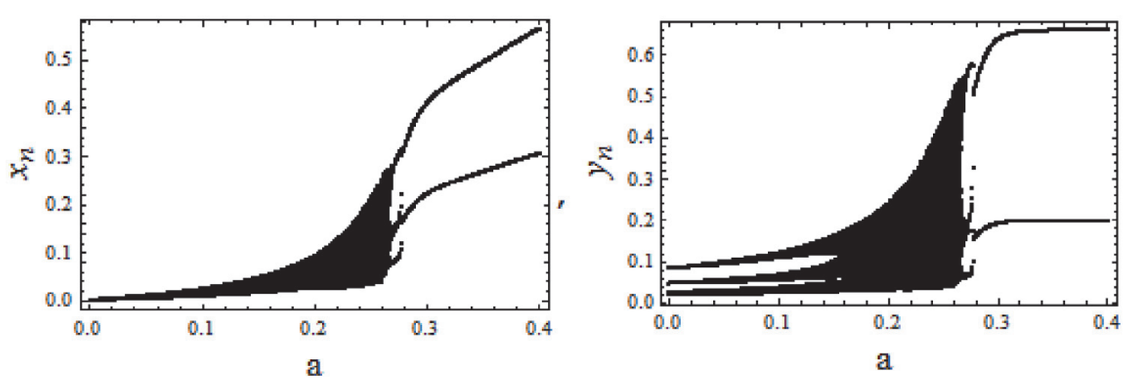

Figure 22.
Bifurcation of map (9) $\alpha = 0.46$, $\beta = 0.7$, $a = 0.16$, $b = 0.6$, $c = 110$ and $0 \leq a \leq 0.4$

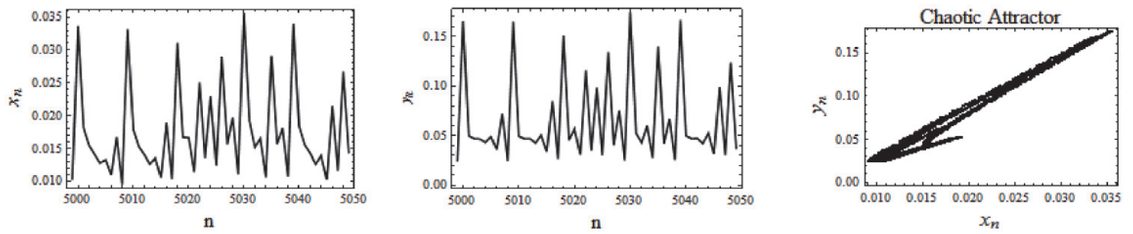

Figure 23.
Time series plots and chaotic attractor of the system (9) for a = 0.16, b = 0.9, c = 105, α = 0.46, β = 0.7 and initial condition (0.1, 0.1).

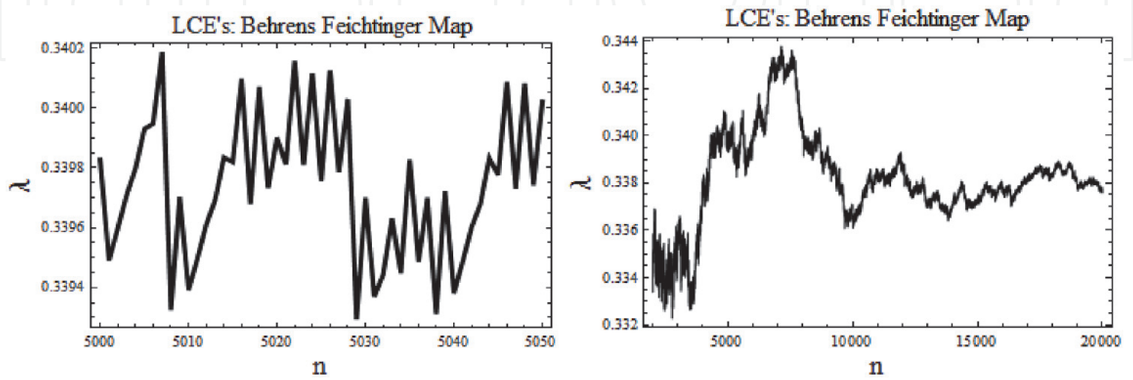

Figure 24.
Plots of Lyapunov exponents for chaotic evolution of the system (9) for a = 0.16, b = 0.9, c = 105, α = 0.46, β = 0.7.

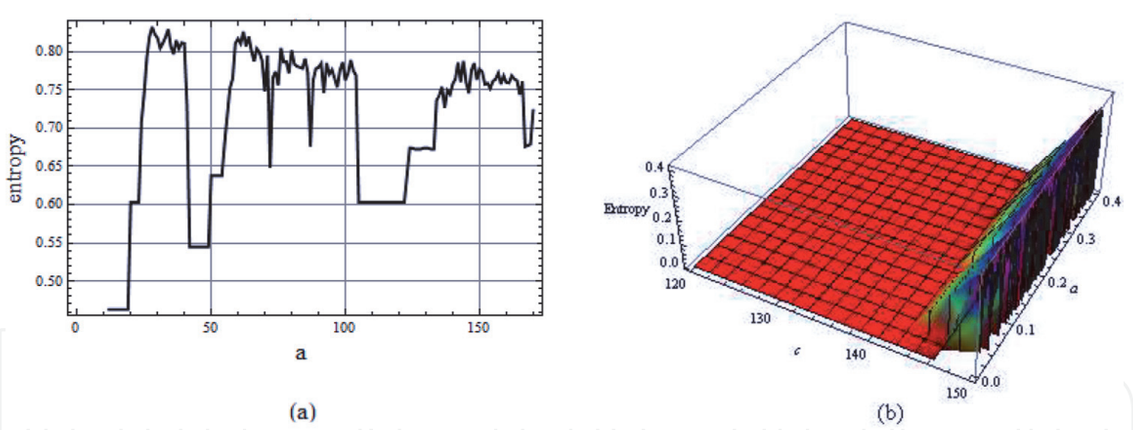

Figure 25.
Plots of topological entropies: (a) left 2D plot is obtained for 12 ≤ c ≤ 170 and values of a = 0.16, b = 0.9, α = *0.46 and* β = *0.7 and (b) right 3D plot is for 120 ≤* c ≤ *150 and 0 ≤* a ≤ *0.4 keeping same values for* α *and* β.

Correlation dimension:

Following steps used for map (8), correlation dimension of chaotic the attractor for values α = 0.46, β = 0.7, a = 0.16, b = 0.9, c = 105, obtained as D_c = 0.064

2.2.3 Continuous Volterra-Petzoldt Model

A continuous 2-dimensional Lotka – Volterra type predator– prey model of constant period chaotic amplitude, (UPCA model), proposed by Petzoldt, [96] based on works, [97, 98], written as

$$\frac{dx}{dt} = a\,x - \alpha_1 \frac{x\,y}{1 + k_1 x}$$

$$\frac{dy}{dt} = -b\,y + \alpha_1 \frac{x\,y}{1 + k_1 x} - \alpha_2 \frac{y\,z}{1 + k_2 y}$$

$$\frac{dz}{dt} = -c(z - w) + \alpha_2 \frac{y\,z}{1 + k_2 y} \tag{10}$$

Bifurcation diagram for predator z while varying prey parameter b shown there, Petzoldt [86], is interesting. Periodic bifurcations and chaotic attractor of this model for different parameter space are presented in the figure, **Figure 26**.

Plots of time series for x(t), for cases of chaos, are given in **Figure 27** and that of Lyapunov exponents, (LCEs), of chaotic attractors shown in last two plots in **Figure 28**.

In conclusion, one observes that the system (10) evolve into chaos after period doubling phenomena.

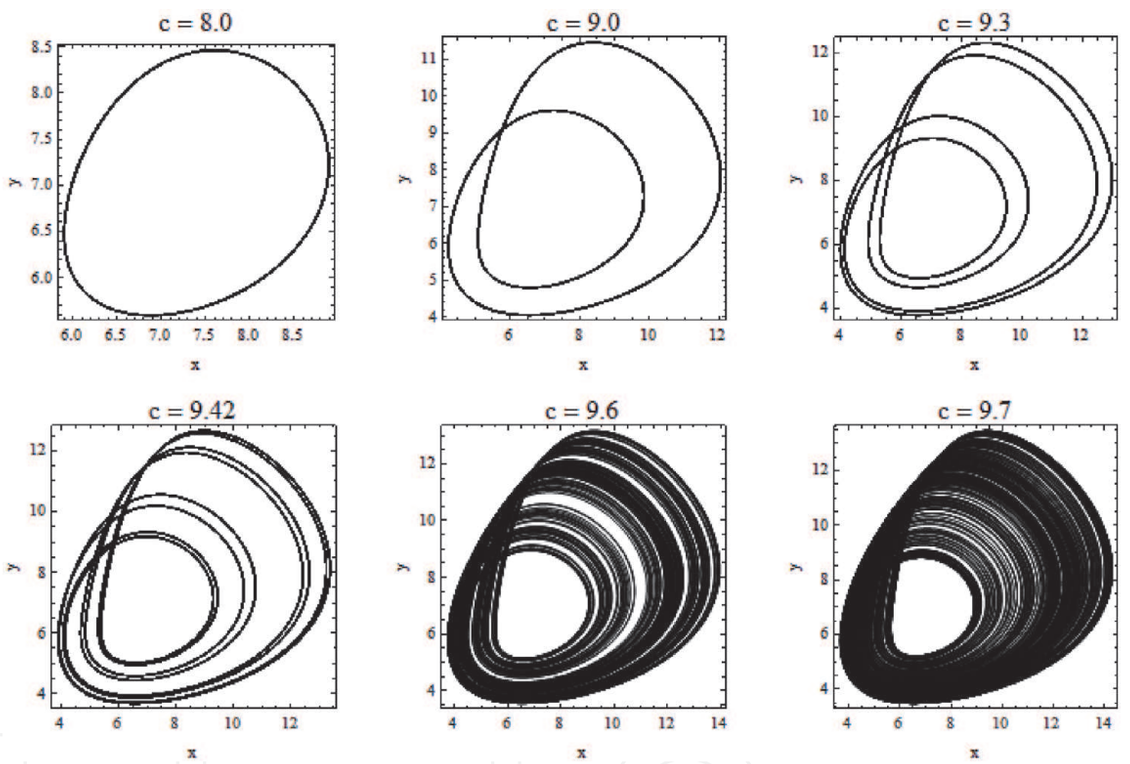

Figure 26.
Periodic bifurcations and chaotic attractor formations of Volterra – Petzoldt model for different values of c fixed parameters $a = 1$, $b = 1$, $\alpha_1 = 0.205$, $\alpha_2 = 1$, $k_1 = 0.05$, $k_2 = 0$, $w = 0.006$.

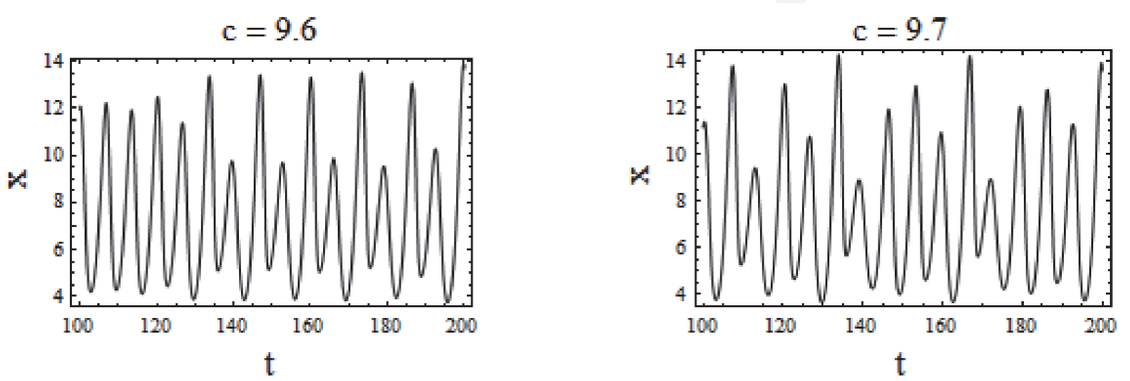

Figure 27.
Plots of time series curves for x(t) for chaotic evolutions for values of c. Other parameters are same as in ***Figure 26****.*

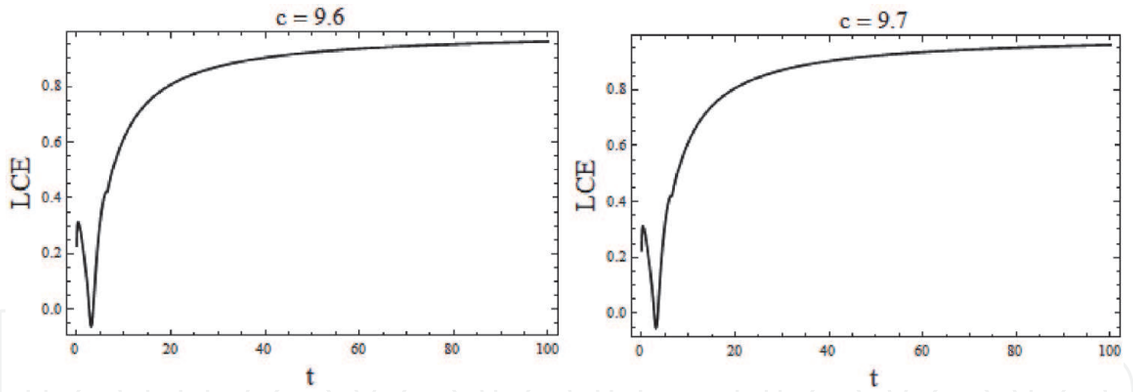

Figure 28.
Plots of LCEs of chaotic attractors of model (1) for values of c. Other parameters are same as in ***Figure 26****.*

3. Chaos control technique

As nonlinear systems are hardly comparable in the sense that behavior of one nonlinear system hardly match with another nonlinear system so the chaotic evolutions. So controlling chaos to bring any chaotic system to regularity may differ from one nonlinear system to another nonlinear system. Different types of controlling chaos technique discussed in recent literatures, [75–88].

Following two chaos controlling technique discussed here:

3.1 Asymptotic Stability Method

Asymptotic stability analysis to stabilize unstable fixed point and to control chaotic motion appeared in some recent researches, [83–85]. Though this method has some limitations, it is perfect way to control chaos in models where it can be applicable.

Description of the Method:

Dynamics of the actual map $\mathbf{X_{n+1}}$ and that of the desired map $\mathbf{Y_{n+1}}$ can be explained by following mapping:

$$\mathbf{X_{n+1}} = \mathbf{F}\left(\mathbf{x_n}, \mathbf{p}\right) \tag{11}$$

$$\mathbf{Y_{n+1}} = \mathbf{F}\left(\mathbf{y_n}, \mathbf{p}*\right) \tag{12}$$

Also, the neighborhood dynamics of $\mathbf{X_{n+1}}$ and $\mathbf{Y_{n+1}}$ can be represented by the relation:

$$\mathbf{X_{n+1}} = \mathbf{A_R X_n} + \mathbf{B_R}\,\mathbf{p}$$

$$\mathbf{Y_{n+1}} = \mathbf{A_D Y_n} + \mathbf{B_D}\,\mathbf{p}*$$

Matrices $\mathbf{A_R}$, $\mathbf{A_D}$, $\mathbf{B_R}$, $\mathbf{B_D}$ can be obtained from the following:

$$\mathbf{A_R} = \mathbf{D_{Xn}}\,\mathbf{F}\left(\mathbf{X_n}, \mathbf{p}\right), \mathbf{A_D} = \mathbf{D_{Yn}}\,\mathbf{F}\left(\mathbf{Y_n}, \mathbf{p}^*\right)$$

$$\mathbf{B_R} = \mathbf{Dp}\,\mathbf{F}\left(\mathbf{X_n}, \mathbf{p}\right), \mathbf{B_D} = \mathbf{Dp}*\mathbf{F}\left(\mathbf{Y_n}, \mathbf{p}^*\right)$$

Here,

$$\mathbf{X_{n+1}} = \begin{pmatrix} x_{n+1} \\ y_{n+1} \end{pmatrix} \mathbf{Y_{n+1}} = \begin{pmatrix} x^*_{n+1} \\ y^*_{n+1} \end{pmatrix}$$

Let a, b are two parameters of the system and (x^n, y^n) be any unstable fixed point of above system for given values of a and b. Then, our objective is to obtain two new values for a and b so that this unstable point becomes stable. For this, we need the Jacobian matrices defined by

$$\mathbf{J} = \begin{pmatrix} \frac{\partial \mathbf{f}}{\partial \mathbf{x}} & \frac{\partial \mathbf{f}}{\partial \mathbf{y}} \\ \frac{\partial \mathbf{g}}{\partial \mathbf{x}} & \frac{\partial \mathbf{g}}{\partial \mathbf{y}} \end{pmatrix}, \ \mathbf{J}^* = \begin{pmatrix} \frac{\partial \mathbf{f}}{\partial \mathbf{a}} & \frac{\partial \mathbf{f}}{\partial \mathbf{b}} \\ \frac{\partial \mathbf{g}}{\partial \mathbf{a}} & \frac{\partial \mathbf{g}}{\partial \mathbf{b}} \end{pmatrix}$$

The control input parameter matrix p*can be given by

$$\mathbf{P}^* = \mathbf{C_R}\,\mathbf{X_n} + \mathbf{C_M}\,\mathbf{p} - \mathbf{C_D}\mathbf{Y_n} \tag{13}$$

Then, using (11)-(13), one obtains the following error equation:

$$\mathbf{e_{n+1}} = (\mathbf{A_R} - \mathbf{B_D}\,\mathbf{C_R})\,\mathbf{e_n} + \{\mathbf{A_R} - \mathbf{A_D} + \mathbf{B_D}(\mathbf{C_D} - \mathbf{C_R})\}\mathbf{Y_n} + (\mathbf{B_R} - \mathbf{B_D}\mathbf{C_M})\mathbf{p} \tag{14}$$

And $\mathbf{e_n} = \mathbf{X_n} - \mathbf{Y_n}$.

Note that in equation (13) and (14) the coefficient matrices $\mathbf{C_R}$, $\mathbf{C_D}$ and $\mathbf{C_M}$ are to be determined so that if the error vector $\mathbf{e_n} = \mathbf{X_n} - \mathbf{Y_n}$ is initialized as $\mathbf{e_0} = \mathbf{0}$, then it will be zero for all n future times. For asymptotic stability, we must have $\mathbf{e_n} \to \mathbf{0}$ as $n \to \infty$, then equation (14) implies

$$\mathbf{A_R} - \mathbf{A_D} + \mathbf{B_D}\,(\mathbf{C_D} - \mathbf{C_R}) = \mathbf{0} = > \mathbf{B_D}(\mathbf{C_D} - \mathbf{C_R}) = \mathbf{A_D} - \mathbf{A_R} \tag{15}$$

$$\text{And } \mathbf{B_R} - \mathbf{B_D}\,\mathbf{C_M} = \mathbf{0} = > \mathbf{B_D}\mathbf{C_M} = \mathbf{B_R} \tag{16}$$

The necessary and sufficient condition for $\mathbf{e_n} \to \mathbf{0}$ as $\mathbf{n} \to \infty$ is

$$\mathbf{A_R} - \mathbf{B_D}\,\mathbf{C_R} = -\mathbf{I} \tag{17}$$

From these, one can obtain matrices $\mathbf{C_M}$, $\mathbf{C_D}$, $\mathbf{C_R}$ and then control parameter matrix $\mathbf{P^*}$ from (13).

A necessary and sufficient condition for the existence of matrices $\mathbf{C_M}$, $\mathbf{C_D}$, $\mathbf{C_R}$, given by:

$$\mathbf{Rank}\,(\mathbf{B_D}) = \mathbf{Rank}\,(\mathbf{B_D}, \mathbf{A_D} - \mathbf{A_R}) = \mathbf{Rank}\,(\mathbf{B_D}, \mathbf{B_R})$$

3.2 Applications

3.2.1 Chaos Control in a 2–Dimensional Prey-Predator map

Considered a prey-predator model where both species evolve with logistic rule and also influencing each other, [30], written as

$$\begin{aligned} x_{n+1} &= a\,x_n(1 - x_n) - b\,x_n\,y_n \\ y_{n+1} &= c\,y_n(1 - y_n) + b\,x_n\,y_n \end{aligned} \tag{18}$$

For $a = 3.7$, $b = 3.5$, $c = 0.2$, one obtains four fixed points obtained as: (0, 0), (0, −4.0), (0.72973, 0) & (0.25712, 0.49961) of which (0.25712, 0.49961) is unstable. So, the orbits originating nearby it would also be unstable and unpredictable & may be chaotic. Nearby this unstable fixed point, we assume a desired initial point as (0.3, 0.5). With this as initial point together with parameters $a = 3.7$, $b = 3.5$,

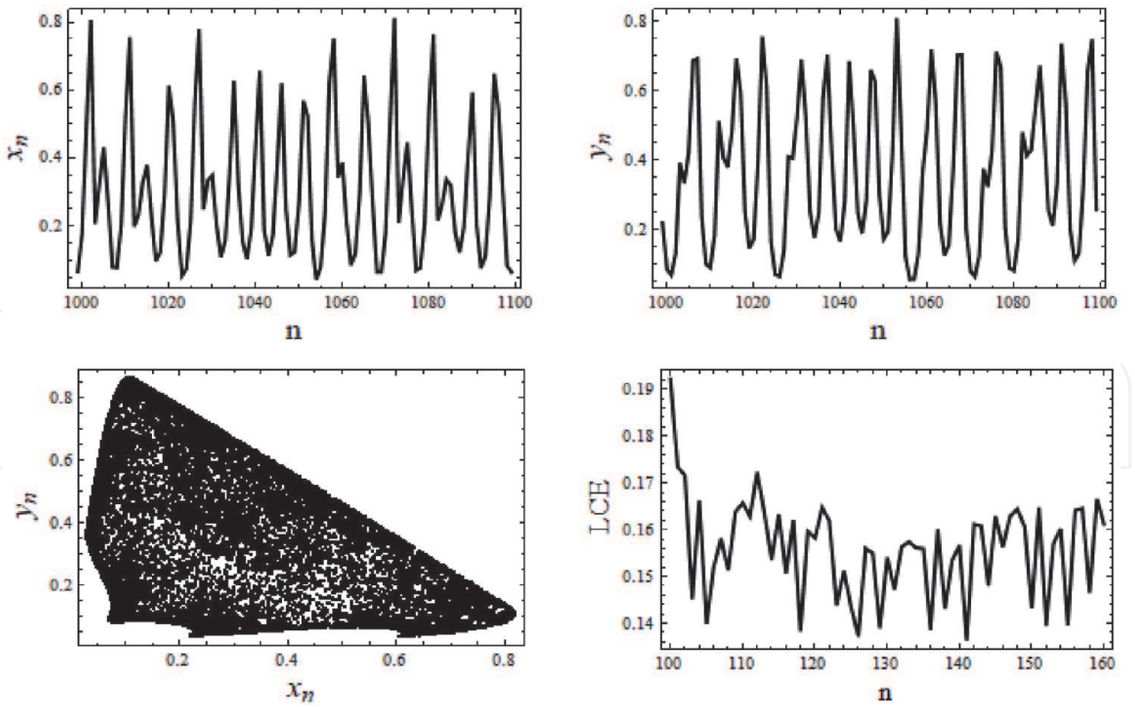

Figure 29.
Time series graphs, attractor and LCE plots of the unstable system.

c = 0.2, time series, attractor and LCE plots are obtained and shown by **Figure 29**. Clearly the system (18) is showing chaos at (0.3, 0.5) with a = 3.7, b = 3.5, c = 0.2.

Then, applying asymptotic stability discussed above for the map (18). For fixed value c = 0.2, unstable fixed point obtained as (0.25712, 0.49961). Nearby this point take initial point (0.3, 0.5) and $\boldsymbol{p}^* = \begin{pmatrix} \boldsymbol{a} \\ \boldsymbol{b} \end{pmatrix} = \begin{pmatrix} 3.7 \\ 3.5 \end{pmatrix}$. When above-mentioned method applied, one obtains matrices:

$$\mathbf{A_R} = \begin{bmatrix} 0.048652 & -0.899924 \\ 1.74865 & 0.900078 \end{bmatrix} \qquad \mathbf{A_D} = \begin{bmatrix} -0.27 & -1.05 \\ 1.75 & 1.05 \end{bmatrix}$$

$$\mathbf{B_R} = \begin{bmatrix} 0.19101 & -0.128462 \\ 0 & 0.128462 \end{bmatrix} \qquad \mathbf{B_D} = \begin{bmatrix} 0.21 & -0.15 \\ 0 & 0.15 \end{bmatrix}$$

$$\mathbf{C_M} = \begin{bmatrix} 0.90957 & 0 \\ 0 & 0.85641 \end{bmatrix} \qquad \mathbf{C_R} = \begin{bmatrix} 3.79669 & -4.76117 \\ 11.6577 & -0.66615 \end{bmatrix}$$

$$\mathbf{C_D} = \begin{bmatrix} 2.28571 & -4.7619 \\ 11.6667 & 0.333333 \end{bmatrix} \qquad \mathbf{p*} = \begin{pmatrix} 3.91525 \\ 2.99538 \end{pmatrix}$$

For the case when c = 0.2; new values of a and b; a = 3.91525, b = 2.99538 along with initial point (0.3, 0.5)a phase plot and a plot of Lyapunov exponents (LEC), are given in **Figure 30**.

3.2.2 Food chain model

Next, we have considered three dimensional food chain model, [23], written as

$$x_{n+1} = a\, x_n(1 - x_n) - b\, x_n y_n$$

$$y_{n+1} = c\, x_n\, y_n - d\, y_n\, z_n$$

$$z_{n+1} = r\, y_n z_n \tag{19}$$

For values $a = 4.1$, $b = 3.7$, $c = 3$, $d = 3.5$, $r = 3.8$ five fixed points exist for system (19) given by: $P_0(0, 0, 0)$, $P_1(0, 0.2632, 0.2857)$, $P_2(0.518614, 0.263158, 0.158812)$, $P_3(0.7561, 0, 0)$ and $P_4(0.3333, 0.4685, 0)$. Then, by stability analysis it has obtained that the fixed points $P_2(0.518614, 0.263158, 0.158812)$ and $P_4(0.3333, 0.4685, 0)$ are unstable. Then, taking nearby P_2, a desired initial point $P^*(0.5, 0.3, 0.2)$, chaotic attractors drawn, **Figure 31**.

In the process of stabilizing the desired point (0.5, 0.3, 0.2), calculations performed to replace parameters $a = 4.1$, $d = 3.5$ and $r = 3.8$ to earlier case of map (18). After obtaining all concerned matrices, replacement matrix obtained as

$$p^* = \begin{pmatrix} a \\ d \\ r \end{pmatrix} = \begin{pmatrix} 4.1035 \\ 1.05194 \\ 1.02707 \end{pmatrix}$$

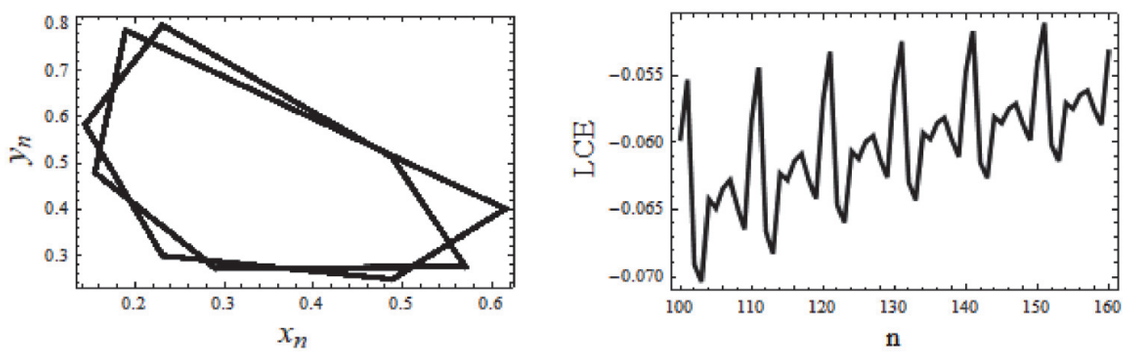

Figure 30.
Phase plot and LCE plot of controlled system when c = 0.2, a = 3.91525, b = 2.99538.

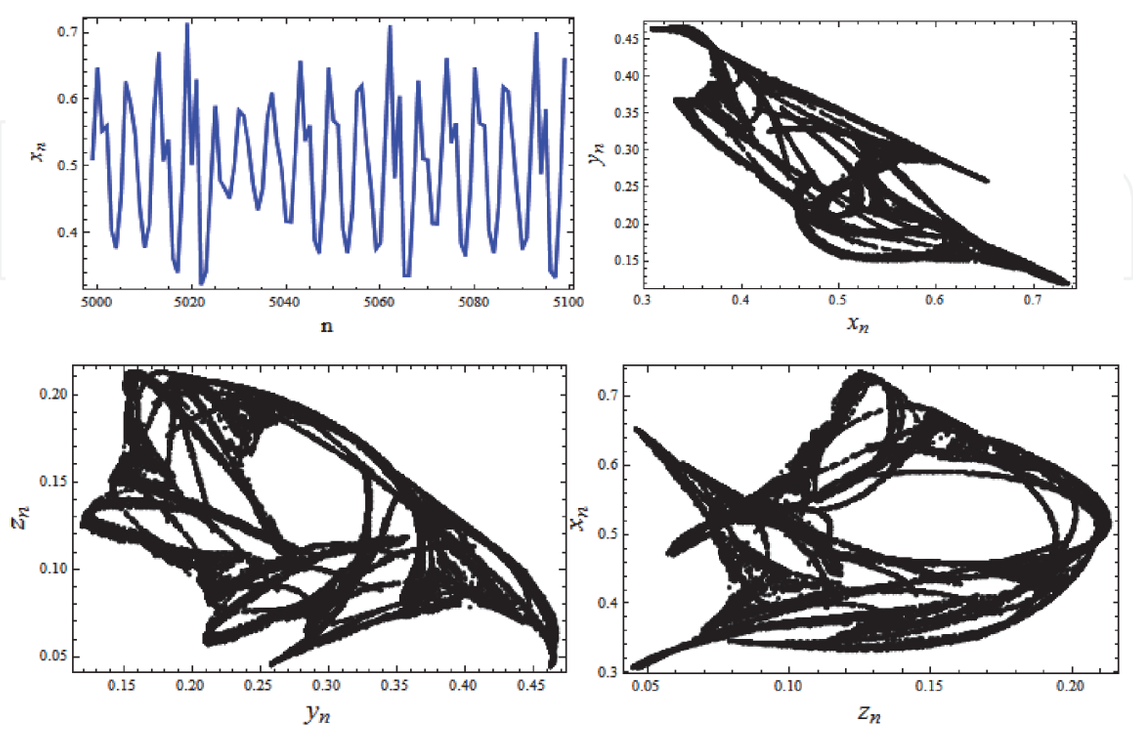

Figure 31.
Time series and attractors of unstable system.

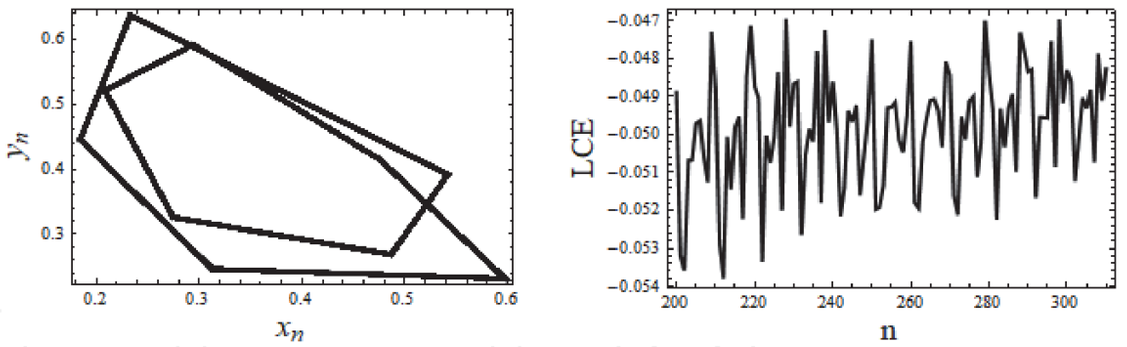

Figure 32.
Phase plot and LCE plot of map (19) showing regular motion and chaos is controlled.

At these new parameter values of a, d and r, the phase plot and the plot of Lyapunov exponents of map (19) obtained, **Figure 32**. These show chaotic motion controlled and the system returns to regularity.

3.2.2.1 Pulsive Feedback Technique to Chaos Control

Pulsive chaos control technique is discussed in detail in recent articles, [86–88]. As an application of this technique let us consider a simple 2 – dimension discrete time Burger's map

3.2.3 Controlling Chaos in 2-D Burger's Map

$$\begin{aligned} x_{n+1} &= (1-a)\,x_n - y_n^2 \\ y_{n+1} &= (1+b)\,y_n + x_n\,y_n \end{aligned} \tag{20}$$

where a and b are non-zero parameters . This map evolve chaotically when a= 0.9, b=0.856. To control chaotic motion we have used pulsive feedback control technique, Litak et al. [86] by

Here $(-0.9, 0.948683)$ is an unstable fixed point of the original Burger's map. It has been observed that above chaotic motion is controlled and display regular behavior after re-writing equations (1) as follows:

$$\begin{aligned} x_{n+1} &= (1-a)\,x_n - y_n^2 + \in (x + 0.9) \\ y_{n+1} &= (1+b)\,y_n + x_n\,y_n + \in (y - 0.948683) \end{aligned} \tag{21}$$

Repeating stability analysis for system (2) with the fixed point $(-0.9, 0.948683)$, one finds this point be stable if $\varepsilon < 0.45$. So, taking $\varepsilon = 0.435$, phase plot obtained as shown in **Figure 34**, indicates chaotic motion, **Figure 33**, is now controlled.

3.2.4 Controlling Chaos in Volterra-Petzoldt Map

Evolution of Volterra-Petzoldt map already discussed in Section 2, Eq. (10). For parameters a = 1, b = 1, c = 9.7, α_1 = 0.205, α_2 = 1, k_1 = 0.05, k_2 = 0 , w = 0.006, this map shows chaotic motion. An unstable equilibrium solution P* (19.5374, 9.64328, 1.02602) exists in this case.

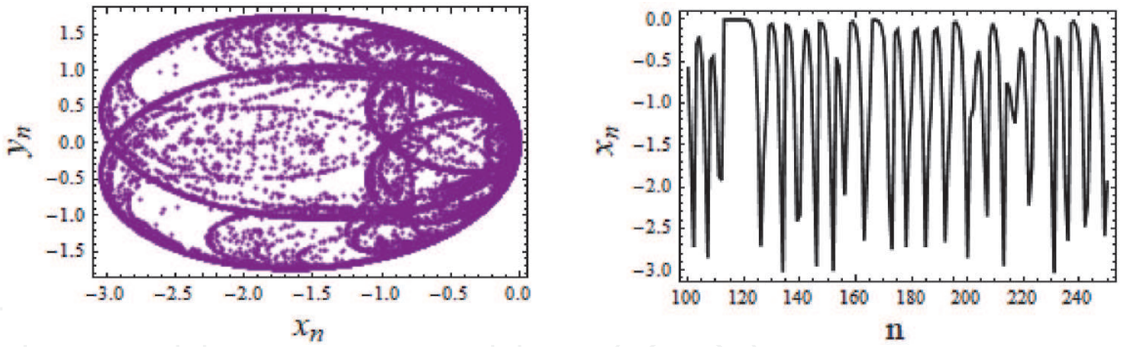

Figure 33.
Chaos in Burgerger's map for a = 1, b = 0.9.

Applying the method of pulsive feedback, and re-writing eq. (10) as

$$\frac{dx}{dt} = a\,x - \alpha_1 \frac{x\,y}{1 + k_1 x} + \in (x - 19.5374)$$

$$\frac{dy}{dt} = -b\,y + \alpha_1 \frac{x\,y}{1 + k_1 x} - \alpha_2 \frac{y\,z}{1 + k_2 y} + \in (y - 9.64328)$$

$$\frac{dz}{dt} = -c(z - w) + \alpha_2 \frac{y\,z}{1 + k_2 y} + \in (z - 1.02602) \qquad (22)$$

Then, using stability analysis, for stabilize the above unstable point P*, one obtains the parameter $\varepsilon = -0.45$.

4. Discussions

Regular and chaotic evolutions observed in some 1-3 dimensional discrete and continuous nonlinear models, which have applications in different areas of science. Presence of complexity in these systems viewed by indications of significant increase in topological entropies in certain parameter spaces. More increase in topological entropy in a system signified the system is more complex. Bifurcation phenomena for different systems show interesting properties like bistability, folding, intermittency, chaos adding etc. which are not common to all nonlinear systems. Proper numerical simulations performed for each system to obtain regular and chaotic attractors, Lyapunov exponents (LCEs) as a measure of chaos, (evolution is regular if LCE < 0 and chaotic if LCE > 0), topological entropies and correlation dimensions for chaotic attractors. It appears from the plots of topological entropies that obtained for discrete models that complexity exists even in absence of chaos. Correlation dimensions obtained for chaotic attractors are non-integers because these attractors bear fractal properties. A chaotic attractor is composed of complex pattern and so, in a variety of nonlinear evolving systems measurement of topological entropy is equally important, [63–67].

To control chaotic motion, techniques of asymptotic stability analysis and that of pulsive feedback control applied here. Pulsive control technique applied to Volterra-Petzoldt map (10) and to Burger's map (20), show chaos successfully controlled and systems returned to regularity, **Figures 34** and **35**. Application of Pulsive control method perfectly controlled chaotic motions in systems (10), (20) shown here. Chaos is also controlled by this method for system (10), [72]. Asymptotic stability analysis method applied to a prey-predator system and to a food chain model, respectively, to maps (18) and (19), and chaos effectively controlled shown,

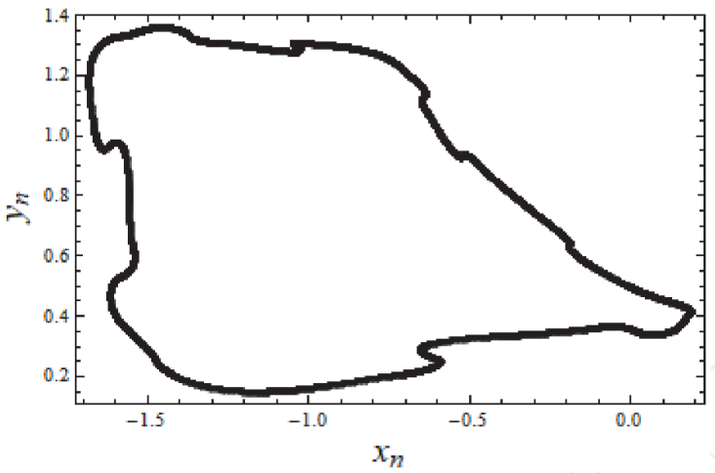

Figure 34.
Plot of regular attractor for a = 1, b = 0.9 and ε = 0.435.

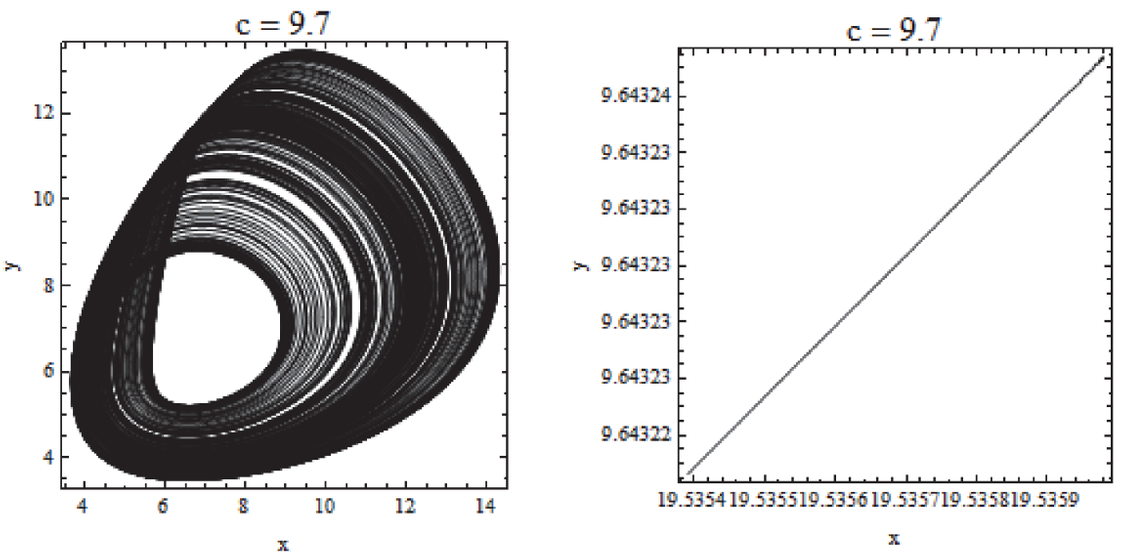

Figure 35.
Plots of chaotic attractor changing into regular attractor by application of pulsive feedback technique.

respectively, through figures, **Figures 30** and **32**. Asymptotic stability analysis technique has some limitations explained in the articles where this method proposed, [83, 84]. Though there are many ways to control chaos in dynamical systems, [74], both the techniques applied here are perfect and very effective in controlling chaos, especially in real systems.

Acknowledgements

The author wishes to present his sincere gratitude to Professor M.K. Das of Institute of Informatics & Communication, University of Delhi South Campus, for his all support and help in preparation of this article.

DOI: http://dx.doi.org/10.5772/intechopen.94295

Author details

Lal Mohan Saha
Department of Mathematics, Shiv Nadar University, Gautam Budha Nagar, India

*Address all correspondence to: lmsaha.msf@gmail.com

References

[1] Poincaré, H. (1957): Les Methodes Nouvelles de la Mecanique Celeste. Dover, New York (1957) Paris, 1899; reprint.

[2] Lorenz EN. Deterministic non-periodic flow. Journal of the Atmospheric Sciences. **1963**;**20**(2): 130-141

[3] Sharkovskii, A. N. (1964).: Co-existence of cycles of a continuous mapping of the line into itself. *Ukrainian Math. J*. **16**: 61–71.

[4] Smale, S.: Differentiable dynamical systems. Bull. Amer. Math. with Soc., 1967; 73 (6), 747–817.

[5] Hènon M. Numerical study of quadratic area-preserving maoings. Quart. J. Math. 1969;**27**:291-311

[6] Ruelle D, Takens F. On the nature of turbulence. Commun. Math. Phys. 1971; **20**:167-192

[7] Guckenheimer, J., Holmes, P. (1971): Nonlinear Oscillations Dynamical Systems, and Bifurcations of Vector Field. Applied Mathematical Sciences, Book Series, Springer.

[8] May RM. Stability and Complexity in Model Ecosystem. Princeton N. J: Princeton University Press; 1974

[9] Li T-Y, Yorke JA. Period Three Implies Chaos. *The American Mathematical Monthly*. 1975. DOI: https://doi.org/10.2307/2318254

[10] May RM. Simple mathematical models with very complicated dynamics. Nature. 1976;**261**:459-467

[11] Rössler OE. An equation for hyperchaos. Physics Letters A. 1979;**71**: 155-157

[12] K. Ikeda, H. Daido and O. Akimoto: Chaotic behavior of transmitted light from a ring cavity. Phys. Rev. Lett., 1980; 45 (9), 709 – 712.

[13] Feigenbaum MJ. Universal behavior in nonlinear systems. Physica. 1983;**7D**: 16-39

[14] Gleick, J. (1987). "Chaos: Making a New Science".

[15] F. C. Moon (1987): Chaotic Vibrations., John Wiley & Sons New York 1987

[16] Devaney RL. An Introduction to Chaotic Dynamical System. Reading: Addison-Wesley; 1989

[17] Ueda Y. Randomly transitional phenomena in the system governed by Duffing's equation. *J. Stat. Phys.* 1979;**20**: 181-196

[18] Stewart I. Does God Play Dice? Penguin Books; 1989

[19] Tanaka Y and Saha LM. (2012): Nonlinear Behaviors of Pulsating Stars with Convective Zones. PASJ**:** Publ. Astron. Soc. Japan 2012;**64**, L8-1- 4.

[20] Lotka AJ. *Elements of Physical Biology*. Baltimore MD: Williams and Wilkins; 1925

[21] Volterra, V. (1931): .*Lecons sur la Thorie Mathmatique de la Lutte pour la Vie*, Gauthiers-Viallars, Paris.

[22] Allee WC. Animal aggregations. *The Quarterly Review of Biology*. 1927;**2**: 367-398

[23] Allee WC, Bowen E. Studies in animal aggregations: mass protection against colloidal silver among goldfishes. Journal of Experimental Zoology. 1932;**61**(2):185-207

[24] Elsadany AA. Dynamical complexities in a discrete-time food chain. *Computational Ecology and Software*. 2012;*2*(2):124-139

[25] Smith M. Mathematical Ideas in Biology. Cambridge: Cambridge University Press; 1968

[26] Freedman HI. Deterministic Mathematical Models in Population Ecology. Marcel Dekker; 1980

[27] J.R. Beddington, C.A. Free and J.H. Lawton. Dynamic complexity in predator–prey models framed in difference equations, Nature. 1975;**255**: 58-60.

[28] Abrams PA, Ginzburg LR. The nature of predation: prey dependent, ratio dependent or neither? Trends in Ecology & Evolution. 2000;**15**(8): 337-341

[29] Grafton, R.Q., Silva-Echenique J. (1994). Predator–Prey Models: Implications for Management. *Atlantic Canada Economics Association Papers 23*, pp. 61–71.

[30] Kaitala V, Heino M. Complex non-unique dynamics in ecological interactions. Proc R Soc London B. 1996; **263**:1011-1015

[31] Quentin Grafton R, Silva-Echenique J. How to manage nature? Strategies, predator-prey models, and chaos. Marine Resource Economics. 1997; **12**(2):127-143

[32] Yakubu A-A. Prey dominance in discrete predator-prey systems with a prey refuge. Mathematical Biosciences. 1997;**144**:155-178

[33] Xiao Y, Cheng D, Tang S. Dynamic complexities in predator–prey ecosystem models with age-structure for predator. *Chaos, Solitons and Fractals*. 2002;**14**:1403-1411

[34] Liu X, Xiao D. Complex dynamic behaviors of a discrete-time predator-prey system. Chaos, Solitons & Fractals. 2007;**32**:80-94

[35] Andrecut, M. and Kauffman, S. A. Chaos in a Discrete Model of a Two-Gene System. Physics Letters A. 2007; 367, 281-287.

[36] Canan C¸ elik, Oktay Duman. Allee effect in a discrete-time predator–prey system. Chaos, Solitons & Fractals, 2009; 40, 1956–1962.

[37] Hadeler KP, Freedman HI. Predator-prey populations with parasitic infection. Journal of Mathematical Biology. 1989;**27**(6):609-631

[38] Danca M, Codreanu S, Bako B. Detailed analysis of a nonlinear predator-prey model. Journal of Biological Physics. 1997;**23**(1):11-20

[39] Wan-Xiong, Yan-Bo-Zhang and Chang-zhong Liu. Analysis of a discrete-time predator-prey system with Allee effect. Ecological Complexity, 2011, 8: 81 – 85.

[40] Zhao M, Yunfei D. Stability of a discrete-time predator-prey system with Allee effect. Nonlinear Analysis and Differential Equations. 2016;**4**(5):225-233

[41] Xian-wei X-l F, Jing Z-j. Dynamics in a discrete-time predator-prey system with Allee effect. Acta Mathematicae Applicatae Sinica. 2013;**20**:143-164

[42] Stephens PA, Sutherland WJ, Freckleton RP. What is the Allee effect? Oikos. 1999;**87**:185-190

[43] Tang S, Chen LA discrete predator–prey system with age-structure for predator and natural barriers for prey. *Mat. Model. Numer. Anal.* 2001;**35**: 675-690

[44] Tang S, Chen L. Density-dependent birth rate, birth pulses and their population dynamic consequences. J. Math. Biol. 2001;**44**(2):185-199

[45] W. Weaver,(1948): "Science and complexity," American Scientist, vol. 36, no. 4, p. 536.

[46] Gribbin, J (2004) Deep Simplicity: Chaos, Complexity and the Emergence of Life. Penguin Press Science.

[47] Simon HA. The architecture of complexity. Proceedings of the American Philosophical Society. 1962; **106**(6):467-482

[48] Gribble, S. 1995, Topological Entropy as a Practical Tool for Identification and Characterization of Chaotic System. Physics 449 Thesis.

[49] Iwai K. Continuity of topological entropy of one dimensional map with degenerate critical points. *J. Math. Sci. Univ. Tokyo*. 1998;**5**:19-40

[50] Hefferman DM. Multistability, intermittency and remerging Feigenbaum trees in an externally pumped ring cavity laser system. *Phys. Lett.* **A**. 1985;**108**:413-422

[51] Walby S. Complexity theory, systems theory, and multiple intersecting social inequalities. Philosophy of the Social Sciences. 2007; **37**(4):449-470

[52] Benettin G, Galgani L, Giorgilli A, Strelcyn JM. Lyapunov Characteristic Exponents for smooth dynamical systems and for Hamiltonian systems; a method for computing all of them. Part 1 & 2: Theory. *Meccanica*. 1980;**15**:9-30

[53] Katok A. Lyapunov exponents, entropy and periodic orbits for diffeomorphisms. *Publ. Math. IHES*. 1980;**51**:137-174

[54] P. Grassberger and Itamar Procaccia. "Measuring the Strangeness of Strange Attractors". Physica D: Nonlinear Phenomena, 1983;9 (1–2): 189–208.

[55] Grassberger P, Procaccia I. Characterization of Strange Attractors. *Physical Review Letters*. 1983;**50**(5): 346-349

[56] Bryant P, Brown R, Abarbanel H. Lyapunov exponents from observed time series. Physical Review Letters. 1990;**65**(13):1523-1526

[57] Brown R, Bryant P, Abarbanel H. Computing the Lyapunov spectrum of a dynamical system from an observed time series. *Phys. Rev. A*. 1991;**43**: 2787-2806

[58] Abarbanel HDI, Brown R, Kennel MB. Local Lyapunov exponents computed from observed data. *Journal of Nonlinear Science*. 1992;**2**(3):343-365

[59] Skokos C. The Lyapunov characteristic exponents and their computation. *Lect. Notes. Phys.* 2009; **790**:63-135

[60] Syta A, Litak G, Budhraja M, Saha LM. Detection of the chaotic behavior of a bouncing ball by 0 – 1 test. **Chaos, Solitons & Fractals**. 2009;**42**: 1511-1517

[61] Adler RL, Konheim AG, McAndrew MH. Topological entropy. Trans. Amer. Math. Soc. 1965;**114**:309-319

[62] Nagashima H, Baba Y. Introduction to Chaos: Physics and Mathematics of Chaotic Phenomena. Overseas Press India Private Limited; 2005

[63] Bowen R. Topological entropy for noncompact sets. Trans. Amer. Math. Soc.1973;184:125-136

[64] Holmes P. 'Strange' phenomena in dynamical systems and their physical

implications. *App. Math. Modelling*. 1977;**7**(1):362-366

[65] P. Holmes (1979) A nonlinear oscillator with a strange attractor, *Phil. Trans. Roy. Soc.Lond.***A 292**(1394): 419 – 448.

[66] Balmforth NJ, Spiegel EA, Tresser C. Topological entropy of one dimenonal maps: approximations and bounds. *Phys. Rev. Lett.* 1994;**72**:80-83

[67] Stewart L, Edward ES. Calculating topological entropy. J. Stat. Phys. 1997; **89**:1017-1033

[68] Yuasa M, Saha LM. Indicators of chaos. Science and Technology, Kinki University. Japan. No. 2008;**20**:1-12

[69] Saha LM, Prasad S and Yuasa M Measuring Chaos: Topological Entropy and Correlation Dimension in Discrete Maps, Science and Technology, Vol. 24, 2012, pg. 10 – 23.

[70] DeCoster GP, Mitchell DW. The efficacy of the correlation dimension technique in detecting determinism in small samples. *Journal of Statistical Computation and Simulation*. 1991;**39**: 221-229

[71] Saha LM, Sharma R. Dynamics of Two-Gene Andrecut-Kauffman System: Chaos and Complexity. Accepted. **Italian Journal of Pure and Applied Mathematica (IJPAM)**. 2018;**41**:405-413

[72] Saha LM, Das MK. Complexities in Micro-Economic Behrens Feichtinger Model. **Indian Journal of Industrial and Applied Mathematics**. 2016;7(2): 127-135

[73] M. Martelli (1999) *Introduction to Discrete Dynamical Systems and Chaos*, Wiley- Interscience

[74] Guanrong Chen and Xiaoning Dong (1998): From Chaos to Order: Methodologies, Perspectives and Applications. World Scientific, Singapore, New Jersey, London, Hong Kong.

[75] Auerbach D, Grebogi C, Ott E, Yorke JA. Controlling chaos in high dimensional systems. Phys. Rev. Lett. 1992;**69**:3479-3482

[76] Erjaee GH, Atabakzade MH, Saha LM. Interesting synchronization-like behavior. **Int. Jour. Bifur.. Chaos**. 2004;**14**(**4**):1447-1453

[77] Carroll TL, Pecora LM. Cascading synchronized chaotic systems. Physica D. 1993;**67**:126-140

[78] Chen G. Optimal control of chaotic systems. Int'l J. of Bifur. Chaos. 1994;**4**: 461-463

[79] Ott E, Grebogi C, Yorke JA. Controlling chaos. Phys. Rev. Lett. 1990; **64**:1196-1199

[80] Pan S, Yin F. Using chaos to control chaotic systems. Phys. Lett. A. 1997;**231**: 173

[81] Pyragas K. Continuous control of chaos by self-controlling feedback. Phys. Lett. A. 1992;**170**:421-428

[82] Shinbrot T, Grebogi C, Ott E, Yorke JA. Using small perturbations to control chaos. Nature. 1993;**363**:411-417

[83] Erjaee GH. On the asymptotic stability of a dynamical system. *IJST, Transaction A*. 2002;***26***(A1):131-135

[84] Saha LM, Erjaee GH and Budhraja M. Controlling chaos in 2-dimensional systems, **Iranian Jour. Sci. Tech.,** Trans. A, 2004;**28**, No.A2, 219 – 226.

[85] Saha LM, Das MK, Bhardwaj R. Asymptotic stability analysis applied to price dynamics. **Ind. J, Industrial and Appl, Math. (IJIAM)**. 2018;**9**(2): 186-195

[86] Litak G, Ali M, Saha LM. Pulsating feedback control for stabilizing unstable periodic orbits in a nonlinear oscillator with a non-symmetric potential. **Int. J. Bifur. Chaos**. 2007;**17**:2797-2803

[87] Litak G, Borowiec M, Ali M, Saha LM, Friswell MI. Pulsive feedback control of a quarter car forced by a road profile. **Chaos Soliton and Fractals**. 2007;**33**:1672-1676

[88] G. Litak, L. M. Saha and M. Ali (2010): Continuous and Pulsive Feedback Control of Chaos, **Recent Progress in Controlling Chaos**, by Miguel A. F. Sanjuan and Celso Grebogi, World Scientific (eBooks), p. 337 – 369.

[89] O'Cairbre F, O'Farrell AG, O'Reilly A. Bistability, bifurcation and chaos in a laser system. *Int. Jour. Bifurcation and Chaos*. 1995;**5**(4):1021-1031

[90] Bonifacio R, Lugiato LA. Bistable absorption in a ring cavity, Lett.l. Nuovo Cimento. 1978;**21**(15):505-510

[91] Benefacio R, Lugato LA. Theory of optical bistability. In: *Dissipative Systems in Quantum Optics*. Ed. R. Benefacio: Springer-Verlag; 1982. pp. 61-92

[92] de Souza SLT, Lima AA, Caldas IL, Medrano-T RO, Guimarães-Filho ZO. Self-similarities of periodic structures for a discrete model of a two-gene system. Physics Letter A. 2012;**376**:1290-1294

[93] Holyst JA, Hagel T, Haag G, Weidlich W. How to control chaotic economy? J. Evol. Econ. 1996;**6**:31-42

[94] Behrens DA. Feichtinger G., Prskawetz A. Complexity dynamics and control of arms race. European Journal of Operational Research, 1997;100: 192-215

[95] Perc M. Microeconomic uncertainties cooperative allince and social welfare. Economics Letters. 2007;**95**:104-109

[96] Thomas Petzoldt (2003): R as a simulation platform in ecological modelling. R. News, Vol. 3/3, 8 – 16.

[97] B. Blasius, A. Huppert and L. Stone. Complex dynamics and phase synchronization in spatially extended ecological systems. Nature, 1999;399: 354 – 359.

[98] Blasius B, Stone L. Chaos and phase synchronization in ecological systems. Int. J. Bifur. And chaos. 2000;**10**: 2361-2380